MICHIGAN STATE UNIVERSITY

CYCLOTRON LABORATORY

BARRIER-TOP RESONANCE AND RESONANT FUSION EXCITATION FUNCTION

N. TAKIGAWA

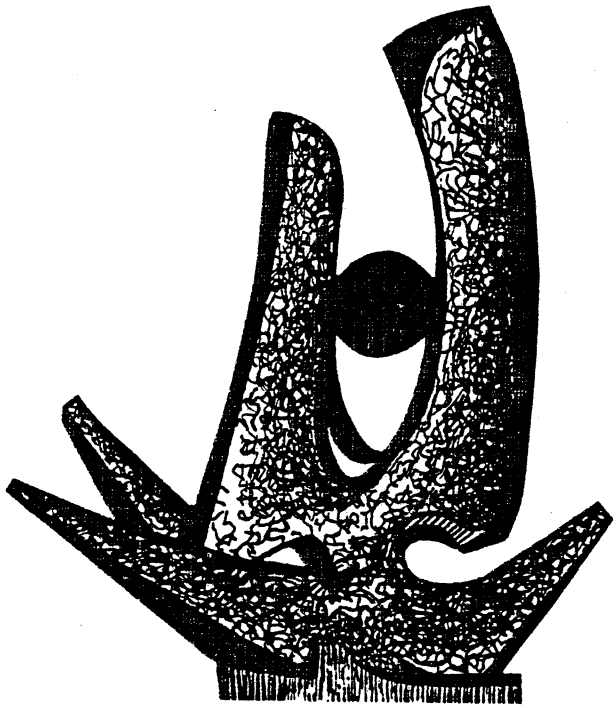

JANUARY 1984

MSUCL-449

MSUCL-449
January 1984

BARRIER-TOP RESONANCE AND RESONANT FUSION EXCITATION FUNCTION

N. Takigawa

National Superconducting Cyclotron Laboratory

and

Department of Physics and Astronomy

Michigan State University, East Lansing, Michigan 48824

Permanent address: Department of Physics, Tohoku University, 980 Sendai, Japan

Talk presented at the Seventh Oaxtepec Symposium on Nuclear Physics, Mexico, January 4-6, 1984.

Abstract

The semi-classical S-matrix is derived for a model of heavy ion collisions in which there are two intrinsic channels with a δ-function coupling at the potential barrier top. The S-matrix reduces to the known result for the resonant scattering from a complex local optical potential when there is no coupling between the relative motion and the intrinsic degrees of freedom. In the case when there exists strong internal absorption, the model exhibits a barrier-top resonance, which has quite different properties from ordinary resonances. We discuss the influence of the barrier-top resonance on the fusion excitation function.

1. Introduction

A number of recent experiments[1-7] have shown that the sub-barrier fusion cross section for medium weight heavy ion collisions is strongly enhanced in comparison with the prediction of a real potential model. Theoretically,[8-16] the enhancement has been attributed to the coupling of the relative motion to intrinsic degrees of freedom, e.g. to the intrinsic vibrational excitations of the colliding nuclei or to particle transfer during the tunneling process. In this talk, I report on the study[17] with G.F. Bertsch concerning a simple model of heavy ion collisions due to S.Y. Lee.[18] The model of the heavy ion collision has two intrinsic channels. It is assumed that the coupling between the relative motion and the intrinsic degrees of freedom is localized at the top of the potential barrier.

We derive semi-classical expressions for the S-matrix, and for the fusion probability. The model contains resonant behaviour which we particularly analyse in this work. The technique we use is an extension of the three turning point semi-classical theory for optical potential scattering[19,20] to the case with explicit coupling to an intrinsic degree of freedom.

In Section 2, we formulate our model. We derive the semi-classical expressions for the S-matrix and for the fusion probability in Section 3. We show that the barrier top δ-function coupling yields a resonance peak in each component of the S-matrix and in the fusion excitation function when there is strong internal absorption. We call this a barrier-top resonance. In Section 4,

we compare the properties of barrier-top resonance to those of ordinary potential resonances. In Section 5, we rederive the semi-classical expression for the fusion excitation function in the presence of strong internal absorption. We introduce the concept of effective channel amplitude through this procedure. A numerical excample is shown in Section 6. The example confirms the arguments in Section 4, and clearly demonstrates the effects of channel coupling on the S-matrix and on the fusion cross section. The dependence of those effects on the reaction Q-value and on the strength of the coupling Hamiltonian are discussed. We summarize the results in Section 7.

2. Two Channel, Barrier-Top δ-Function Coupling Model

A two channel model can be conveniently formulated by using Pauli's spin matrices. The Schrödinger equation which we wish to solve is

$$\left\{-\frac{\hbar^2}{2\mu}\frac{d^2}{dr^2}+U(r)\right\}\begin{pmatrix}1&0\\0&1\end{pmatrix}\Psi+\begin{pmatrix}E_{int}^{(1)}&0\\0&E_{int}^{(2)}\end{pmatrix}\Psi+\lambda f(r)\,\sigma_x\Psi=E\begin{pmatrix}1&0\\0&1\end{pmatrix}\Psi \qquad (2.1)$$

where $E_{int}^{(i)}$ is the intrinsic energy of the i-th channel, and

$$\sigma_x=\begin{pmatrix}0&1\\1&0\end{pmatrix} \qquad (2.2)$$

We consider a limiting case when the inelastic excitation or the transfer reaction occurs only at the barrier top position R_B. Accordingly, we express the coupling form factor f(r) as

$$f(r)=\delta(r-R_B) \qquad (2.3)$$

This enables us to write down explicitly the semi-classical S-matrix, using known expansion formulae for the Whittaker functions.[21,22] In eq. (2.1), the potential U(r) can be complex so as to take into account the effects which are not explicitly described by the two channel model, i.e. by the last term on the left hand side of eq. (2.1).

3. Semi-Classical S-Matrix and the Fusion Probability

3.1. DERIVATION OF THE SEMI-CLASSICAL S-MATRIX

3.1.1. Wave function

We obtain an approximate form of the wave function by using the method of the comparison equation[23] (see Appendix A). We use a linear and a quadratic comparison function for the inner and the external regions of the potential barrier, respectively. The external region contains the potential barrier region. With the δ-function interaction, the linear momentum makes a sudden change at the barrier top position R_B. We therefore divide the whole space into three regions (see Fig. 1). Region I lies outside of R_B. Region II covers from R_B inward to some internal domain. Region III is the most internal region.

There are three classical turning points in each channel (see Fig. 1). They are in general complex numbers. We denote them $r_1^{(i)}$, $r_2^{(i)}$, and $r_3^{(i)}$, where the upper suffix i refers to the channel 1 or 2, respectively. $r_1^{(i)}$ and $r_2^{(i)}$ are the external turning points, which appear on the right hand side and on the left hand side of the potential barrier, respectively. The $r_3^{(i)}$ is the most internal turning point. This notation is the extension

to the two channel problem of the notation of ref. 19. Using the channel wave functions defined in Appendix B, the wave function in each region can be expressed as follows.

In region I

$$\Psi_I(r) = \begin{pmatrix} A_{IW}^{(R1)}\,\Psi_{IW}^{(R)}(E_1,r) + A_{OW}^{(R1)}\,\Psi_{OW}^{(R)}(E_1,r) \\ A_{IW}^{(R2)}\Psi_{IW}^{(R)}(E_2,r) + A_{OW}^{(R2)}\,\Psi_{OW}^{(R)}(E_2,r) \end{pmatrix} \tag{3.1}$$

where E_i is the energy of relative motion in channel i, i.e.

$$E_i = E - E_{int}^{(i)} \tag{3.2}$$

The upper suffix R refers to the right hand side of the potential barrier. The channel wave functions have been constructed to have the following asymptotic behaviour when r is well outside of the barrier region,

$$\begin{pmatrix} \Psi_{IW}^{(R)}(E_i,r) \\ \Psi_{OW}^{(R)}(E_i,r) \end{pmatrix} \sim \frac{1}{\sqrt{2}}[\chi_i(r)]^{-\frac{1}{4}} \begin{pmatrix} e^{-i[S_1^{(i)}(r) - \frac{1}{2}\epsilon_i \ln \epsilon_i - \frac{\pi}{4}]} \\ e^{i[S_1^{(i)}(r) - \frac{1}{2}\epsilon_i \ln \epsilon_i - \frac{\pi}{4}]} \end{pmatrix} \tag{3.3}$$

where $\chi_i(r)$ is the square of the local wave number in channel i, and $S_j^{(i)}(r)$ and ϵ_i are given by

$$S_j^{(i)}(r) = \int_{r_j^{(i)}}^{r} [\chi_i(r)]^{\frac{1}{2}}\, dr \tag{3.4}$$

and

$$\epsilon_i = \frac{i}{\pi} \int_{r_1^{(i)}}^{r_2^{(i)}} [\chi_i(r)]^{\frac{1}{2}}\, dr \tag{3.5}$$

In the following, we use also the following notation,

$$S_{jk}^{(i)} = \int_{r_j^{(i)}}^{r_k^{(i)}} [\chi_i(r)]^{1/2}\, dr \qquad (3.6)$$

The boundary condition is

$$A_{IW}^{(22)} = 0 \qquad (3.7)$$

In region II, the wave function is given by

$$\psi_{II}(r) = \begin{pmatrix} A_{IW}^{(11)}\ \psi_{IW}^{(L)}(E_1,r) + A_{0W}^{(L1)}\ \psi_{0W}^{(L)}(E_1,r) \\ A_{IW}^{(12)}\ \psi_{IW}^{(L)}(E_2,r) + A_{0W}^{(L2)}\ \psi_{0W}^{(L)}(E_2,r) \end{pmatrix} \qquad (3.8)$$

where the upper suffix L refers to the left hand side of the potential barrier. The basic wave functions have been constructed to have the following asymptotic form when r is well inside of the potential barrier

$$\begin{pmatrix} \psi_{IW}^{(L)}(E_i,r) \\ \psi_{0W}^{(L)}(E_i,r) \end{pmatrix} \sim \frac{1}{\sqrt{2}}[\chi_i(r)]^{-1/4} \begin{pmatrix} e^{-i[S_2^{(i)}(r)+\frac{1}{2}\xi_i \ln \xi_i/e - \frac{\pi}{4}]} \\ e^{i[S_2^{(i)}(r)+\frac{1}{2}\xi_i \ln \xi_i/e - \frac{\pi}{4}]} \end{pmatrix} \qquad (3.9)$$

The wave function in region III has to be regular at the origin. This boundary condition and the linear comparison function leads to

$$\psi_{III}(r) = \begin{pmatrix} A_{III}^{(1)} \left(\frac{d\sigma^{(1)}}{dr}\right)^{-1/2} Ai\left(-\{\sigma^{(1)} - \sigma_3^{(1)}\}\right) \\ A_{III}^{(2)} \left(\frac{d\sigma^{(2)}}{dr}\right)^{-1/2} Ai\left(-\{\sigma^{(2)} - \sigma_3^{(2)}\}\right) \end{pmatrix} \qquad (3.10)$$

where the coordinate in the comparison equation $\sigma^{(i)}$ is related to the original coordinate r through the mapping equation which conserves the action integral, i.e.

$$\frac{2}{3}(\sigma^{(i)} - \sigma_3^{(i)})^{3/2} = \int_{r_3^{(i)}}^{r} [\chi_i(r)]^{1/2}\, dr \qquad (3.11)$$

When r is far to the right of the most internal turning point $r_3^{(i)}$, the asymptotic behaviour of the Airy function together with the mapping relation eq. (3.11) leads to the following asymptotic expression,

$$\psi_{II}(r) \sim \frac{1}{\sqrt{\pi}} \begin{pmatrix} A_{III}^{(1)}[\chi_1(r)]^{-1/4} \frac{1}{2i}\left\{e^{i[S_3^{(1)}(r)+\frac{\pi}{4}]} - e^{-i[S_3^{(1)}(r)+\frac{\pi}{4}]}\right\} \\ A_{III}^{(2)}[\chi_2(r)]^{-1/4} \frac{1}{2i}\left\{e^{i[S_3^{(2)}(r)+\frac{\pi}{4}]} - e^{-i[S_3^{(2)}(r)+\frac{\pi}{4}]}\right\} \end{pmatrix} \qquad (3.12)$$

3.1.2. Matching of the wave function

In order to find the matching condition between the wave functions ψ_{III} and ψ_{II}, we rewrite the asymptotic expression of ψ_{III} in terms of $S_2^{(i)}(r)$ instead of $S_3^{(i)}(r)$. The result reads,

$$\psi_{III}(r) \sim \frac{1}{2\sqrt{\pi}} \begin{pmatrix} A_{III}^{(1)}[\chi_1(r)]^{-1/4}\left\{e^{iS_{32}^{(1)}} e^{i[S_2^{(1)}(r)-\frac{\pi}{4}]} + e^{-iS_{32}^{(1)}} e^{-i[S_2^{(1)}(r)-\frac{\pi}{4}]}\right\} \\ A_{III}^{(2)}[\chi_2(r)]^{-1/4}\left\{e^{iS_{32}^{(2)}} e^{i[S_2^{(2)}(r)-\frac{\pi}{4}]} + e^{-iS_{32}^{(2)}} e^{-i[S_2^{(2)}(r)-\frac{\pi}{4}]}\right\} \end{pmatrix} \qquad (3.13)$$

Comparing eq. (3.13) with eqs. (3.8) and (3.9), we obtain

$$\begin{pmatrix} A_{IW}^{(Li)} \\ A_{0W}^{(Li)} \end{pmatrix} = \frac{A_{III}^{(i)}}{\sqrt{2\pi}} \begin{pmatrix} e^{i\frac{1}{2}\xi_i \ln \xi_i/e}\ e^{-iS_{32}^{(i)}} \\ e^{-i\frac{1}{2}\xi_i \ln \xi_i/e}\ e^{iS_{32}^{(i)}} \end{pmatrix} \qquad (3.14)$$

The matching condition between the wave functions ψ_I and ψ_{II} can be obtained by a simple extension of the procedure for the one dimensional scattering problem from a δ-function potential. The requirement of continuity of the wave function across R_B leads to

$$\begin{pmatrix} A_{IW}^{(R1)}\psi_{IW}^{(R)}(E_1,R_B)+A_{OW}^{(R1)}\psi_{OW}^{(R)}(E_1,R_B) \\ A_{IW}^{(R2)}\psi_{IW}^{(R)}(E_2,R_B)+A_{OW}^{(R2)}\psi_{OW}^{(R)}(E_2,R_B) \end{pmatrix} = \begin{pmatrix} A_{IW}^{(L1)}\psi_{IW}^{(L)}(E_1,R_B)+A_{OW}^{(L1)}\psi_{OW}^{(L)}(E_1,R_B) \\ A_{IW}^{(L2)}\psi_{IW}^{(L)}(E_2,R_B)+A_{OW}^{(L2)}\psi_{OW}^{(L)}(E_2,R_B) \end{pmatrix} \tag{3.15}$$

The second condition, which is associated with the momentum change at R_B, is obtained by integrating eq. (2.1) over an infinitesimal region encompassing R_B. This leads to

$$\begin{pmatrix} -\frac{\hbar^2}{2\mu_1}\left\{A_{IW}^{(R1)}\dot{\psi}_{IW}^{(R)}(E_1,R_B)+A_{OW}^{(R1)}\dot{\psi}_{OW}^{(R)}(E_1,R_B)-A_{IW}^{(L1)}\dot{\psi}_{IW}^{(L)}(E_1,R_B)-A_{OW}^{(L1)}\dot{\psi}_{OW}^{(L)}(E_1,R_B)\right\} \\ -\frac{\hbar^2}{2\mu_2}\left\{A_{IW}^{(R2)}\dot{\psi}_{IW}^{(R)}(E_2,R_B)+A_{OW}^{(R2)}\dot{\psi}_{OW}^{(R)}(E_2,R_B)-A_{IW}^{(L2)}\dot{\psi}_{IW}^{(L)}(E_2,R_B)-A_{OW}^{(L2)}\dot{\psi}_{OW}^{(L)}(E_2,R_B)\right\} \end{pmatrix}$$

$$+\lambda\begin{pmatrix} A_{IW}^{(L2)}\psi_{IW}^{(L)}(E_2,R_B)+A_{OW}^{(L2)}\psi_{OW}^{(L)}(E_2,R_B) \\ A_{IW}^{(L1)}\psi_{IW}^{(L)}(E_1,R_B)+A_{OW}^{(L1)}\psi_{OW}^{(L)}(E_1,R_B) \end{pmatrix}=0 \tag{3.16}$$

We next introduce a (4 x 4) transition matrix T,

$$\begin{pmatrix} A_{IW}^{(R1)} \\ A_{OW}^{(R1)} \\ A_{IW}^{(R2)} \\ A_{OW}^{(R2)} \end{pmatrix} = \begin{pmatrix} & & & \\ & T & & \\ & & & \end{pmatrix} \begin{pmatrix} A_{IW}^{(L1)} \\ A_{OW}^{(L1)} \\ A_{IW}^{(L2)} \\ A_{OW}^{(L2)} \end{pmatrix} \tag{3.17}$$

Then, eqs. (3.15), (3.16), and the expansion formulae of the Whittaker function at the origin[22] give us

$$(T)=\begin{pmatrix} D_1 & O_{12} \\ O_{21} & D_2 \end{pmatrix} \tag{3.18a}$$

where

$$D_i=\begin{pmatrix} \frac{1}{t_i} & e^{\pi\varepsilon_i} \\ e^{\pi\varepsilon_i} & t_i(1+e^{2\pi\varepsilon_i}) \end{pmatrix} \tag{3.18b}$$

and

$$O_{ij}=\begin{pmatrix} \nu_i f(\varepsilon_i,\varepsilon_j)/t_j & \nu_i f(\varepsilon_i,\varepsilon_j)(e^{\pi\varepsilon_i}+e^{-\frac{\pi}{2}i}) \\ \nu_i f(\varepsilon_j,\varepsilon_i)(e^{\pi\varepsilon_i}+e^{-\frac{\pi}{2}i}) & \nu_i f(\varepsilon_j,\varepsilon_i)t_j(e^{\pi\varepsilon_i}+e^{-\frac{\pi}{2}i})(e^{\pi\varepsilon_j}+e^{-\frac{\pi}{2}i}) \end{pmatrix} \tag{3.18c}$$

In eq. (3.18), t_i is the bare tunneling amplitude in channel i, and is given by,

$$t_i=\frac{e^{-\frac{1}{2}\pi\varepsilon_i}}{\sqrt{2\pi}}\Gamma\left(\tfrac{1}{2}+i\varepsilon_i\right) \tag{3.19a}$$

$$=\frac{1}{\sqrt{1+e^{2\pi\varepsilon_i}}}e^{i\arg\Gamma\left(\frac{1}{2}+i\varepsilon_i\right)} \tag{3.19b}$$

Our tunneling amplitude t is related to the barrier penetration factor N(iε) of ref. 19 as,

$$N(i\varepsilon_i)=\frac{1}{t(\varepsilon_i)}e^{-\pi\varepsilon_i}e^{i\varphi_i} \tag{3.20}$$

where

$$\varphi_i=\varepsilon_i\ln\varepsilon_i/e \tag{3.21}$$

ν_1 and ν_2 are the scaled coupling strength, and are given by

$$\nu_1 = \lambda \, \xi_{12} \tag{3.22a}$$

$$\nu_2 = \lambda \, \xi_{21} \tag{3.22b}$$

$$\xi_{kl} = \tfrac{1}{2} k^{-3/2} \mu_k^{1/4} \mu_l^{-1/4} (\Lambda_k \Lambda_l)^{-1/4} \tag{3.22c}$$

where μ_i and Ω_i are the reduced mass and the curvature of the potential barrier in channel i, respectively. The latter is given by

$$\Lambda_i = \left(\left| \frac{\hbar^2}{\mu_i} \frac{d^2}{dr^2} U_i(r) \right| / \mu_i \right)^{1/2} \tag{3.23}$$

In the following, we shall assume identical Hamiltonians in the two channels, i.e. $\mu_1 = \mu_2$, $U_1(r) = U_2(r) = U(r)$, $\Omega_1 = \Omega_2$, and hence $\nu_1 = \nu_2 = \nu$.

The quantity f is defined as

$$f(\xi_1, \xi_2) = e^{\frac{\pi}{4} i} \, e^{\frac{\pi}{4}(\xi_1 - \xi_2)} 2^{-\frac{1}{2} i (\xi_1 - \xi_2)} \frac{\Gamma\left(\frac{1}{4} + i \frac{\xi_2}{2}\right)}{\Gamma\left(\frac{3}{4} + i \frac{\xi_1}{2}\right)} \tag{3.24}$$

It has the following symmetry property,

$$f(\xi_1, \xi_2) \xi_1 = f(\xi_2, \xi_1) \xi_2 \tag{3.25}$$

3.1.3. Wave propagation matrices

The wave propagation matrix method[20] offers a way to derive the semiclassical S-matrix in a physically transparent and systematic way.

Let us express the wave function in the external asymptotic region as,

$$\psi \sim \begin{pmatrix} C_{IW}^{(1)} & C_{OW}^{(1)} & C_{IW}^{(2)} & C_{OW}^{(2)} \end{pmatrix} \begin{pmatrix} \vartheta_c^{(1)}(r) \\ \theta_c^{(1)}(r) \\ \vartheta_c^{(2)}(r) \\ \theta_c^{(2)}(r) \end{pmatrix} \tag{3.26}$$

where $I_c^{(i)}(r)$ and $O_c^{(i)}(r)$ are the incoming and outgoing scattering solutions[19] of the Coulomb potential in channel i. We prefer the (1 x 1), scalar expression of the wave function given by eq. (3.26) to a (2 x 1) vector expression,

$$\psi = \begin{pmatrix} C_{IW}^{(1)} \vartheta_c^{(1)}(r) + C_{OW}^{(1)} \theta_c^{(1)}(r) \\ C_{IW}^{(2)} \vartheta_c^{(2)}(r) + C_{OW}^{(2)} \theta_c^{(2)}(r) \end{pmatrix} \tag{3.27}$$

The scalar expression is more convenient in connection with the wave propagation matrix method.

The wave propagation matrices connect the amplitudes of the channel wave functions in various domains as follows

$$\begin{pmatrix} C_{IW}^{(1)} \\ C_{OW}^{(1)} \\ C_{IW}^{(2)} \\ C_{OW}^{(2)} \end{pmatrix} = \begin{pmatrix} \Delta \end{pmatrix} \begin{pmatrix} \Phi \end{pmatrix} \begin{pmatrix} A_{IW}^{(R1)} \\ A_{OW}^{(R1)} \\ A_{IW}^{(R2)} \\ A_{OW}^{(R2)} \end{pmatrix} \tag{3.28}$$

$$\begin{pmatrix} A_{IW}^{(R1)} \\ A_{OW}^{(R1)} \\ A_{IW}^{(R2)} \\ A_{OW}^{(R2)} \end{pmatrix} = \begin{pmatrix} T \end{pmatrix} \begin{pmatrix} A_{IW}^{(L1)} \\ A_{OW}^{(L1)} \\ A_{IW}^{(L2)} \\ A_{OW}^{(L2)} \end{pmatrix} \tag{3.29}$$

and

$$\begin{pmatrix} A_{IW}^{(L1)} \\ A_{OW}^{(L1)} \\ A_{IW}^{(L2)} \\ A_{OW}^{(L2)} \end{pmatrix} = \begin{pmatrix} \quad \\ \quad \Phi \quad \\ \quad \end{pmatrix} \begin{pmatrix} \quad \\ \quad S \quad \\ \quad \end{pmatrix} \begin{pmatrix} A_m^{(1)}/\sqrt{2\pi} \\ A_m^{(1)}/\sqrt{2\pi} \\ A_m^{(2)}/\sqrt{2\pi} \\ A_m^{(2)}/\sqrt{2\pi} \end{pmatrix} \tag{3.30}$$

Eq. (3.26) can then be rewritten as

$$\psi \sim \frac{1}{\sqrt{2\pi}} \left(A_m^{(1)} A_m^{(1)} A_m^{(2)} A_m^{(2)} \right) V \left(J_c^{(1)}(r) \; 0_c^{(1)}(r) \; J_c^{(2)}(r) \; 0_c^{(2)}(r) \right)^T \tag{3.31}$$

where V is a (4 x 4) matrix given by

$$V = S^T \Phi^T T^T \Phi^T \Delta^T \tag{3.32}$$

In eqs. (3.31) and (3.32), the transpose of a matrix A is denoted by A^T.

Eq. (3.14) leads to the following expression for the matrices Φ and S,

$$(\Phi) = \begin{pmatrix} e^{i\frac{1}{2}\varphi_1} & 0 & 0 & 0 \\ 0 & e^{-i\frac{1}{2}\varphi_1} & 0 & 0 \\ 0 & 0 & e^{i\frac{1}{2}\varphi_2} & 0 \\ 0 & 0 & 0 & e^{-i\frac{1}{2}\varphi_2} \end{pmatrix} \tag{3.33}$$

$$(S) = \begin{pmatrix} e^{-iS_{32}^{(1)}} & 0 & 0 & 0 \\ 0 & e^{iS_{32}^{(1)}} & 0 & 0 \\ 0 & 0 & e^{-iS_{32}^{(2)}} & 0 \\ 0 & 0 & 0 & e^{iS_{32}^{(2)}} \end{pmatrix} \tag{3.34}$$

where ϕ_i is given by eq. (3.21). The matrices S and Φ represent the additional phase factor obtained by the wave function when the wave propagates from the most internal turning point r_3 to the middle turning point r_2 and from r_2 to the barrier top position R_B, respectively. The matrix T describes the rearrangement of the wave function and is given by eq. (3.18). In Eq. (3.28), the matrix Φ represents the additional phase factor obtained by the wave function when the wave further propagates from R_B to the most external turning point r_1. It is also given by eq. (3.33). The matrix Δ represents the nuclear phase shift evaluated from the most external turning point, and is given by

$$(\Delta) = \begin{pmatrix} e^{-i\delta_1^{(1)}} & 0 & 0 & 0 \\ 0 & e^{i\delta_1^{(1)}} & 0 & 0 \\ 0 & 0 & e^{-i\delta_1^{(2)}} & 0 \\ 0 & 0 & 0 & e^{i\delta_1^{(2)}} \end{pmatrix} \tag{3.35}$$

where

$$\delta_1^{(i)} = \int_{r_1^{(i)}}^{R} [\chi_i(r)]^{1/2} \, dr - \int_{r_c^{(i)}}^{R} [\chi_i^{(c)}(r)]^{1/2} \, dr \tag{3.36}$$

In eq. (3.36), $r_c^{(i)}$ is the Coulomb turning point in channel i, $\chi_i^{(c)}(r)$ is the squared wave number in the absence of the nuclear potential, and R is any point outside the range of the nuclear interaction.

3.1.4. Semiclassical S-matrix

The scattering boundary condition is that the coefficient of $I_c^{(2)}(r)$ in eq. (3.31) is zero. This leads to,

$$A^{(1)}_{III} = - A^{(1)}_{III} \, (V_{13} + V_{23}) / (V_{33} + V_{43}) \tag{3.37}$$

The S-matrix elements are then given by

$$\eta_{11} = \frac{(V_{12}+V_{22})(V_{33}+V_{43}) - (V_{32}+V_{42})(V_{13}+V_{23})}{(V_{11}+V_{21})(V_{33}+V_{43}) - (V_{31}+V_{41})(V_{13}+V_{23})} \tag{3.38}$$

and

$$\eta_{12} = \frac{(V_{14}+V_{24})(V_{33}+V_{43}) - (V_{34}+V_{44})(V_{13}+V_{23})}{(V_{11}+V_{21})(V_{33}+V_{43}) - (V_{31}+V_{41})(V_{13}+V_{23})} \tag{3.39}$$

Using the wave propagation matrices given in Sec. 3.1.3, eqs. (3.38) and (3.39) become,

$$\eta_{11} = \frac{e^{2i\delta_1^{(1)}}}{N(i\varepsilon_1)} \frac{\left\{1+\bar{N}(i\varepsilon_1) e^{2i S_{32}^{(1)}}\right\}\left\{1+\frac{e^{2i S_{32}^{(2)}}}{N(i\varepsilon_2)}\right\} - \nu_1\nu_2 f(\varepsilon_1,\varepsilon_2) f(\varepsilon_2,\varepsilon_1)(1+e^{-\frac{\pi}{2}i} e^{-\pi\varepsilon_1}) g(\varepsilon_1) g(\varepsilon_2)}{\left\{1+\frac{e^{2i S_{32}^{(1)}}}{N(i\varepsilon_1)}\right\}\left\{1+\frac{e^{2i S_{32}^{(2)}}}{N(i\varepsilon_2)}\right\} - \nu_1\nu_2 f(\varepsilon_1,\varepsilon_2) f(\varepsilon_2,\varepsilon_1) g(\varepsilon_1) g(\varepsilon_2)} \tag{3.40}$$

and

$$\eta_{12} = \frac{e^{i(\delta_1^{(1)}+\delta_1^{(2)})}}{N(i\varepsilon_1)} \frac{\nu_2 f(\varepsilon_1,\varepsilon_2) e^{\frac{1}{2}i(\vartheta_1-\vartheta_2)} e^{-\frac{\pi}{2}i} e^{-\pi\varepsilon_1} g(\varepsilon_1) g(\varepsilon_2)}{\left\{1+\frac{e^{2i S_{32}^{(1)}}}{N(i\varepsilon_1)}\right\}\left\{1+\frac{e^{2i S_{32}^{(2)}}}{N(i\varepsilon_2)}\right\} - \nu_1\nu_2 f(\varepsilon_1,\varepsilon_2) f(\varepsilon_2,\varepsilon_1) g(\varepsilon_1) g(\varepsilon_2)} \tag{3.41}$$

where

$$g(\varepsilon_i) = 1 + (1 + e^{-\frac{\pi}{2}i} e^{-\pi\varepsilon_i}) e^{2i S_{32}^{(i)}} \frac{1}{N(i\varepsilon_i)} \tag{3.42}$$

and

$$\bar{N}(i\varepsilon_i) = \frac{\sqrt{2\pi}}{\Gamma(\frac{1}{2}-i\varepsilon_i)} e^{-\frac{\pi}{2}\varepsilon_i} e^{-i\varepsilon_i \ln \varepsilon_i/e} \tag{3.43a}$$

$$= t(\varepsilon_i)(1+e^{2\pi\varepsilon_i}) e^{-\pi\varepsilon_i} e^{-i\varepsilon_i \ln \varepsilon_i/e} \tag{3.43b}$$

3.2. REDUCTION TO A ONE-CHANNEL PROBLEM

Eqs. (3.40) and (3.41) are the generalization of the semi-classical S-matrix obtained in ref. 19 for the scattering from a complex optical potential. They reduce to the result in ref. 19 when the coupling is set equal to zero. As has been discussed previously [19], the resulting elastic scattering S-matrix η_{el} can be decomposed into two components, which describe physically different scattering processes, i.e.

$$\eta_{el} = \frac{e^{2i\delta_1}}{N(i\varepsilon)} \frac{1+\bar{N}(i\varepsilon) e^{2i S_{32}}}{1+\frac{e^{2i S_{32}}}{N(i\varepsilon)}} \tag{3.44}$$

$$= \eta_B + \eta_I \tag{3.45}$$

where

$$\eta_B = \eta_B^{(0)} / N(i\varepsilon) \tag{3.46}$$

with

$$\eta_B^{(0)} = e^{2i\delta_1} \tag{3.47}$$

and

$$\eta_I = \eta_I^{(0)} \cdot h \tag{3.48}$$

with

$$\eta_I^{(1)} = \frac{e^{2i\delta_3}}{[N(i\varepsilon)]^2} \tag{3.49}$$

and

$$h = \frac{1}{1 + \frac{e^{2i\,S_{32}}}{N(i\varepsilon)}} \tag{3.50}$$

The η_B describes the waves which are reflected around the external potential barrier. The η_I describes waves which penetrate inside the potential well and are reflected by the most internal turning point r_3. They are called the barrier and the internal wave S-matrices. Eq. (3.47) is the usual WKB formula for one turning point. The factor N in eq. (3.46) is the reflection amplitude when the incident waves encounter the potential barrier from the right hand side. Compared to the barrier wave S matrix, the one step internal wave S-matrix $\eta_I^{(0)}$ has an additional phase corresponding to the optical path length of a round trip from the external turning point r_1 to the internal turning point r_3. The reflection, or the transmission, factor N appears twice in eq. (3.49), because the internal waves encounter the potential barrier twice. The factor h describes the effect of multiple reflection of waves inside the potential pocket, and causes an enhancement of the internal wave cross section when resonances occur.

3.3. UNITARITY IN THE ABSENCE OF INTERNAL ABSORPTION

If there is no absorption, the S-matrix has to satisfy the unitarity condition. It is quite easy to prove unitarity in

single channel problems. For example, if the incident energy is below the potential barrier, then ε is a positive real number. One can then prove that

$$\bar{N}(i\varepsilon) = N^*(i\varepsilon) \tag{3.51}$$

Moreover, all the action integrals are real, so that eq. (3.44) immediately leads to

$$|\eta_{ll}| = 1 \,. \tag{3.52}$$

It is not so easy to prove the unitarity in the two channel problem in general. Still, if we consider the case when the incident energy is below the potential barrier, unitarity in the incident channel can be proved by using the following relationship,

$$f^*(\varepsilon_1,\varepsilon_2) = f(\varepsilon_2,\varepsilon_1)\, e^{\pi(\varepsilon_1-\varepsilon_2)} \frac{1 + e^{-\frac{\pi}{2}i} e^{-\pi\varepsilon_1}}{1 + e^{\frac{\pi}{2}i} e^{-\pi\varepsilon_2}} \tag{3.53}$$

3.4. S-MATRIX AND THE FUSION PROBABILITY IN THE PRESENCE OF STRONG INTERNAL ABSORPTION

Let us now consider the case where there is strong internal absorption in both channels 1 and 2. In this case $S_{32}^{(1)}$ and $S_{32}^{(2)}$ carry large positive imaginary parts[19]. One can therefore set the factors including these quantities equal to zero in eqs. (3.40) and (3.41). The resultant S-matrix reads

$$\eta_{11} = \frac{e^{2i\delta_1^{(1)}}}{N(i\varepsilon_1)} \frac{1 - \nu_1\nu_2 f(\varepsilon_1,\varepsilon_2) f(\varepsilon_2,\varepsilon_1)\left(1 + e^{-\frac{\pi}{2}i} e^{-\pi\varepsilon_1}\right)}{1 - \nu_1\nu_2 f(\varepsilon_1,\varepsilon_2) f(\varepsilon_2,\varepsilon_1)} \tag{3.54}$$

and

$$\eta_{12} = \frac{e^{i(\delta_1^{(0)}+\delta_1^{(2)})}}{N(\varepsilon_1,\varepsilon_2)} \frac{\nu_2 f(\varepsilon_1,\varepsilon_2)\, e^{i\frac{1}{2}(\eta_1-\eta_2)}\, e^{-\frac{\pi}{2}i}\, e^{-\pi\varepsilon_1}}{1-\nu_1\nu_2 f(\varepsilon_1,\varepsilon_2) f(\varepsilon_2,\varepsilon_1)} \tag{3.55}$$

This η_{11} is a generalization of the barrier wave S-matrix η_B.

The fusion probability P is given by

$$P = 1 - |\eta_{11}|^2 - |\eta_{12}|^2 . \tag{3.56}$$

In order to derive a formula to calculate P, we assume that there is no absorption in the barrier region, i.e. we assume that ε_1 and ε_2 are real positive numbers. Using eqs. (3.20), (3.54), and (3.55), we then obtain

$$P = P_1^{(0)} \cdot \zeta \tag{3.57}$$

where $P_1^{(0)}$ is the bare tunneling probability in the entrance channel. It is given by

$$P_1^{(0)} = |t_1|^2 . \tag{3.58}$$

The factor ζ carries the meaning of an enhancement factor of the tunneling probability due to coupling to an intrinsic degree of freedom. It is given by

$$\zeta = \frac{1 + |f(\varepsilon_1,\varepsilon_2)|^2 \nu^2}{|1 - \nu^2 f(\varepsilon_1,\varepsilon_2) f(\varepsilon_2,\varepsilon_1)|^2} \tag{3.59}$$

4. Properties of the Barrier-Top Resonance

Eqs. (3.54) and (3.55) indicate that there occurs a resonance when the following condition is satisfied in a system having strong internal absorption,

$$1 - \nu^2 f(\varepsilon_1,\varepsilon_2) f(\varepsilon_2,\varepsilon_1) = 0 \tag{4.1}$$

The occurrence of a resonance is associated with the fact that the one dimensional δ-function potential-well has a bound state. This can be easily confirmed in a degenerate two channel model (see Appendix C). The resonance appears at the place where the δ-function coupling form factor is set, i.e. at $r = R_B$ in the present model given by eq. (2.3). Let us call this resonance a barrier-top resonance.

There is one and only one barrier-top resonance for a given value of the coupling strength, since there is only one bound state in the one dimensional δ-function potential. In order to obtain information concerning the position and the width of the resonance from eq. (4.1), we consider a degenerate model in which the reaction Q-value is zero. We introduce a complex energy $E - i\frac{1}{2}\Gamma$, and expand the action integral ε with respect to $(\frac{1}{2}\Gamma + V_I)$, V_I being the strength of the imaginary part of the optical potential. Up to first order, this leads to

$$\varepsilon = \int_{r_2}^{r_1} k(r)\, dr + i\left(\tilde{V}_I^{(B)} + \tfrac{1}{2}\Gamma\right) \tau_{21}/\hbar \tag{4.2}$$

where

$$K(r) = \left[\frac{2\mu}{\hbar^2}(V_R(r) - E)\right]^{\frac{1}{2}} = \frac{\mu v^{(B)}(r)}{\hbar} \tag{4.3}$$

$$\tau_{21} = \int_{r_2}^{r_1} \frac{dr}{v^{(B)}(r)} \tag{4.4}$$

and

$$\tilde{V}_I^{(B)} = \int_{r_2}^{r_1} U_I(r)\,\frac{dr}{v^{(B)}(r)} \Big/ \tau_{21} \qquad (4.5)$$

In eqs. (4.3) and (4.5), $U_R(r)$ and $U_I(r)$ are the real and the imaginary parts of the optical potential, respectively. In eqs. (4.2) through (4.5), we have dropped the suffix to distinguish channels 1 and 2. Here, $v^{(B)}(r)$ is the local velocity in the barrier region, and τ_{21} is the transmission time across the potential barrier. Also, $\tilde{V}_I^{(B)}$ is the average strength of the absorption in the barrier region. We use Stirling's formula for the gamma functions in the factor f. This is accurate when the incident energy is well below the potential barrier so that the absolute value of ε is large. We then obtain the following formulae from eq. (4.1),

$$\frac{1}{2} R_e \zeta - \frac{1}{\hbar} \int_{r_2}^{r_1} k(r)\,dr = \nu \qquad (4.6)$$

and

$$\frac{1}{2}\Gamma = \frac{\hbar}{\tau_{21}} - \tilde{V}_I^{(B)} \qquad (4.7)$$

Note that for a parabolic potential barrier

$$\varepsilon = (V_B - E)/\hbar\Omega \ , \qquad (4.8)$$

where V_B is the barrier top energy, and $\hbar\Omega$ is the curvature of the potential barrier given by eq. (3.23).

In order to demonstrate the characteristics of the barrier-top resonance, let us compare eqs. (4.1), (4.6), and (4.7) with the corresponding equations for an ordinary potential resonance

in a one dimensional scattering problem. The resonance condition for the potential resonance is (see eq. (3.44)),

$$N(i\zeta) + e^{2iS_{32}} = 0 \qquad (4.9)$$

Similarly to eq. (4.2), we expand the action integral S_{32} up to the first order of $\frac{1}{2}\Gamma + V_I$,

$$S_{32} = \int_{r_3}^{r_2} k(r)\,dr - i\left(\tilde{V}_I^{(I)} + \frac{1}{2}\Gamma\right)\tau_{32}/\hbar \qquad (4.10)$$

where

$$k(r) = \left(\frac{2\mu}{\hbar^2}(E - U_R(r))\right)^{1/2} = \frac{\mu v^{(I)}(r)}{\hbar} \qquad (4.11)$$

$$\tau_{32} = \int_{r_3}^{r_2} \frac{dr}{v^{(I)}(r)} \qquad (4.12)$$

and

$$\tilde{V}_I^{(I)} = \int_{r_3}^{r_2} U_I(r)\,\frac{dr}{v^{(I)}(r)} \Big/ \tau_{32} \qquad (4.13)$$

Here $v^{(I)}(r)$ is the local velocity in the internal region and τ_{32} is the traversal time across the potential pocket. Also, $\tilde{V}_I^{(I)}$ is the average strength of the absorption in the internal region. Eqs. (4.9) and (4.10) lead to,

$$S_{32} = \left(n + \frac{1}{2}\right)\pi + \frac{1}{2}\varphi_N \quad (n = 0, 1, 2, \cdots\cdots) \qquad (4.14)$$

and

$$\frac{1}{2}\Gamma = \frac{\hbar}{\tau_{32}} \ln|N| - \tilde{V}_I^{(I)} \qquad (4.15a)$$

where ϕ_N is the phase of factor N. If the resonance energy is well below the barrier top energy, then (see eqs. (3.20) and (3.19b)),

$$\ln |N| = \ln \sqrt{1+e^{-2\pi\xi}} \approx \frac{1}{2} e^{-2\pi\xi} \qquad (4.16)$$

In this limit, eq. (4.15a) can be rewritten as

$$\frac{1}{2}\Gamma \approx \frac{\hbar}{2\tau_{3\ell}} e^{-2\pi\xi} - \tilde{V}_I^{(I)} \qquad (4.15b)$$

Eq. (4.14) is essentially a Bohr-Sommerfeld quantization condition, though it is adapted so as to take into account the property of the potential barrier. On the other hand, eqs. (4.6) and (4.8) suggest that the energy of the barrier-top resonance is uniquely determined by the strength of the coupling Hamiltonian. The energy shift from the barrier top energy is expected to be proportional to the square of the strength of the coupling Hamiltonian.

The widths of barrier-top resonances have unusual properties. Although eqs. (4.7) and (4.15b) show that the width of both the barrier-top resonance and the ordinary potential resonance consists of two parts, i.e. the width due to absorption (the second term) and the width due to leakage through the potential barrier, there are two distinct differences between their widths. The coefficient of the transmission time is a factor of two smaller for the barrier-top resonance than for the potential resonance. This is because the waves inside the potential well must make a round trip inside the well to encounter the potential barrier, whereas the wave

associated with the barrier-top resonance needs to traverse only one way, either to the right or to the left.

We also find that the leakage width of the barrier-top resonance is not reduced by the transmission probability factor. Namely, eq. (4.7) does not contain the factor $e^{-2\pi\varepsilon}$, which appears in eq. (4.15b). We can therefore expect that the barrier-top resonance will have much broader width than the ordinary potential resonance, at least as far as the leakage width is concerned, and that the width of the barrier-top resonance changes with the resonance position much more slowly than in the case of the potential resonances. The property that the leakage width of the barrier-top resonance does not contain the transmission probability factor seems to be consistent with the structure of the semiclassical S-matrix given by eq. (3.45). Both of them suggest that the transmission probability is one where the waves cross a boundary between a classically allowed and a classically forbidden region from the side of the classically forbidden region. Note that the turning point r_2 appears always as an intermediate point in eq. (3.45).

We wish to comment that the barrier-top resonance introduced in this work is different from the barrier-top resonance discussed in ref. 24. The latter was discussed in a one dimensional potential scattering problem, and has nothing to do with the coupling to intrinsic degrees of freedom. It is associated with the zeroes of the factor N in eq. (3.46). Eqs. (3.20) and (3.19) then show that the corresponding resonance position is obtained from the singularity points of the gamma function as,

$$\frac{1}{2} + i\xi = -n \qquad (n = 0, 1, 2 \cdots\cdots) \qquad (4.17)$$

Hence,

$$E = V_B \quad \text{and} \quad \tfrac{1}{2}\Gamma = -V_I + \hbar\Lambda(n+\tfrac{1}{2}) \tag{4.18}$$

This is a kind of Bohr-Sommerfeld quantization condition (anti-Bohr-Sommerfeld condition!).

5. Fusion Excitation Function in the Presence of Strong Internal Absorption

Inelastic excitation or particle transfer might cause a significant effect on the fusion excitation function. In the present model, the effect is described by the enhancement factor ζ in eq. (3.57), for the case of strong internal absorption. In this section, we rederive eq. (3.57) by using the incoming wave boundary condition. This method conveniently decomposes the total fusion cross section into two components, each of which has clear physical meaning.

In the incoming wave boundary condition model, the total wave function on the left hand side of the potential barrier is assumed to be,

$$\psi_L(r) = \begin{pmatrix} A_{IW}^{(L1)}\ \psi_{IW}^{(L)}(E_1, r) \\ A_{IW}^{(L2)}\ \psi_{IW}^{(L)}(E_2, r) \end{pmatrix} \tag{5.1}$$

This has to be matched to the wave function on the right hand side of the potential barrier given by

$$\psi_R(r) = \begin{pmatrix} A_{IW}^{(R1)}\psi_{IW}^{(R)}(E_1, r) + A_{OW}^{(R1)}\psi_{OW}^{(R)}(E_1, r) \\ A_{OW}^{(R2)}\ \psi_{OW}^{(R)}(E_2, r) \end{pmatrix} \tag{5.2}$$

The matching conditions read,

$$\begin{pmatrix} A_{IW}^{(R1)}\psi_{IW}^{(R)}(E_1, R_B) + A_{OW}^{(R1)}\psi_{OW}^{(R)}(E_1, R_B) \\ A_{OW}^{(R2)}\ \psi_{OW}^{(R)}(E_2, R_B) \end{pmatrix} = \begin{pmatrix} A_{IW}^{(L1)}\ \psi_{IW}^{(L)}(E_1, R_B) \\ A_{IW}^{(L2)}\ \psi_{IW}^{(L)}(E_2, R_B) \end{pmatrix} \tag{5.3}$$

and

$$\begin{pmatrix} -\frac{\hbar^2}{2\mu_1}\left\{A_{IW}^{(R1)}\dot{\psi}_{IW}^{(R)}(E_1, R_B) + A_{OW}^{(R1)}\dot{\psi}_{OW}^{(R)}(E_1, R_B) - A_{IW}^{(L1)}\dot{\psi}_{IW}^{(L)}(E_1, R_B)\right\} \\ -\frac{\hbar^2}{2\mu_2}\left\{A_{OW}^{(R2)}\dot{\psi}_{OW}^{(R)}(E_2, R_B) - A_{IW}^{(L2)}\dot{\psi}_{IW}^{(L)}(E_2, R_B)\right\} \end{pmatrix} + \lambda \begin{pmatrix} A_{IW}^{(L2)}\psi_{IW}^{(L)}(E_2, R_B) \\ A_{IW}^{(L1)}\psi_{IW}^{(L)}(E_1, R_B) \end{pmatrix} = 0 \tag{5.4}$$

Note that R_B is mapped on $\sigma = 0$ in the comparison equation using a quadratic comparison function (see Appendix A). Using the expansion formulae of the Whittaker functions around the origin, we then obtain,

$$A_1 \equiv \frac{A_{IW}^{(L1)}}{A_{IW}^{(R1)}} = t_1 \frac{1}{1 - \nu^2 f(E_1, E_2) f(E_2, E_1)} = t_1 \cdot h_1 \tag{5.5}$$

and

$$A_2 \equiv \frac{A_{IW}^{(L2)}}{A_{IW}^{(R1)}} = -t_1 \cdot \nu \cdot \frac{f(E_1, E_2)}{1 - \nu^2 f(E_1, E_2) f(E_2, E_1)} \tag{5.6a}$$

$$= -t_2 \cdot \nu \cdot \frac{f(E_2, E_1)}{1 - \nu^2 f(E_1, E_2) f(E_2, E_1)} \tag{5.6b}$$

$$= -t_2 \cdot h_2 \tag{5.6c}$$

The quantity A_i is the transmission amplitude in channel i. It is given as a product of the transmission amplitude through a one dimensional potential barrier in channel i, and the effective amplitude to be in that channel, effective channel amplitude, h_i. It is easy to show that eqs. (5.5) and (5.6) recover eq. (3.57). These equations have been first derived by S.Y. Lee in ref. 18. An important discovery in ref. 18 is that the sum of the square of the effective channel amplitudes is not necessarily equal to 1, i.e.

$$|h_1|^2 + |h_2|^2 \neq 1 \tag{5.7}$$

Actually, $|h_1|$ far exceeds 1 in a sub-barrier region, and both of $|h_1|$ and $|h_2|$ exhibit a peak at the energy corresponding to a barrier-top resonance. Accordingly, the enhancement factor ζ also shows a resonance peak. These will be exemplified in the next section.

6. Numerical Example

In order to numerically demonstrate the results of the previous sections, we consider here an extreme example. Namely, we consider here a scattering from a parabolic potential barrier in the presence of δ-function coupling at the barrier top position. We assume that all the waves which have passed the barrier region are completely absorbed (the incoming wave boundary condition), and that there is no absorption around the barrier region. The formulae derived in the previous sections show that we need to specify only the values of the curvature of the potential barrier

$\hbar\Omega$, of the reaction Q-value, $Q = E^{(1)}_{int} - E^{(2)}_{int}$, and of the coupling strength v. Throughout the following calculations, we choose $\hbar\Omega$ to be 4 MeV. This is a reasonable value for describing heavy ion collisions.

Fig. 2 shows the absolute values of the S matrix elements as functions of the incident energy for three different coupling strengths. The Q-value is fixed to be zero for all calculations. The thin and the thick lines represent $|\eta_{11}|$ and $|\eta_{12}|$, respectively. One clearly observes a resonance extremum in each S matrix element for a given coupling strength. Note that the change of the resonance width is small as the resonance position moves with the coupling strength. In fact, the change is much slower than what one would expect from the energy dependence of the transmission probability. This numerically supports the peculiar property of the barrier-top resonance with respect to its width, discussed in Sec. 4. The value of the extremum is 0.5. This can be explained as follows. The resonance condition eq. (4.1) is an equation in the complex plane, so that it has two components. Since we calculate the S-matrix for real values of energy, these two conditions cannot be simultaneously satisfied. Instead, only the following condition is satisfied when the incident energy coincides with the real part of the resonance energy, which is complex,

$$1 = v \, \mathrm{Re}\, f(\epsilon, \epsilon) \tag{6.1}$$

One can prove that the following formulae hold at the energy where eq. (6.1) is fulfilled,

$$\eta_{11} = \frac{1}{2} e^{i[2\delta_1^{(1)} - \varphi_N - \varphi]} \tag{6.2a}$$

and

$$\eta_{12} = \frac{1}{2} e^{i[\delta_1^{(1)} + \delta_1^{(2)} - \varphi_N]} \tag{6.2b}$$

where ϕ_N is the phase of the factor N and ϕ is given by

$$\varphi = \tan^{-1}(e^{-\pi\epsilon}) \tag{6.3}$$

We thus obtain

$$|\eta_{11}| = |\eta_{12}| = 1/2 \tag{6.4}$$

This mechanism resembles the following mechanism of the appearance of the minima of Regge zeroes in the S-matrix[25]) in standard optical model calculations. The absolute value of the total S-matrix for an optical potential scattering shows minima of Regge zeroes when one of the resonance conditions, i.e. the Bohr-Sommerfeld quantization condition, is satisfied in the standard calculations using real energy and real angular momentum.

Fig. 3 shows the dependence of the resonance energy on the strength of the coupling Hamiltonian. Based on the arguments in the previous paragraph, the resonance energy has been assigned to the incident energy, for which the S-matrix elements take extrema for a given ν^2. The dot-dashed line is the prediction of the semi-classical formula eq. (4.6). It nicely reproduces the trend

of the results of the numerical calculations. Fig. 4 shows the dependence of the absolute value of the S-matrix elements on the reaction Q-value. The strength of the coupling Hamiltonian has been fixed to be $\nu^2 = 0.4$. The thin and the thick lines represent $|\eta_{11}|$ and $|\eta_{12}|$, respectively. The numbers designate the reaction Q-value in units of MeV. We clearly observe resonance extrema in both $|\eta_{11}|$ and $|\eta_{12}|$.

Fig. 5 shows the excitation function of the fusion cross section for five different coupling strengths. For comparison, the fusion excitation function in the absence of coupling is also shown (a thick monotonic line). Roughly speaking, one finds that the channel coupling strongly enhances the sub-barrier fusion cross section and slightly reduces the fusion cross section above the barrier. In addition, we see clear resonance phenomena. Fig. 6 shows the effective channel amplitude of the entrance channel as a function of the incident energy for five different coupling strengths. The reaction Q-value is set at zero for all calculations. As has been first pointed out in ref. 18, $|h_1|$ alone far exceeds unity in the sub-barrier region. It shows also a clear resonance peak for each coupling strength. Similarly to Fig. 2, Figs. 5 and 6 confirm the argument in Sec. 4 that the width of the barrier-top resonance does not depend much on the resonance energy.

Fig. 7 compares the fusion excitation function in the presence of channel coupling with the bare fusion excitation function. The coupling strength for the thick lines is $\nu^2 = 0.4$. The Q-

value in the thick solid, dot-dashed and dashed lines is +4.0 MeV, 0 MeV, and -4.0 MeV, respectively. One observes that the sub-barrier fusion cross section is enhanced overall, regardless of the sign of the reaction Q-value. This is to be expected if one recognizes that the large enhancement of the sub barrier fusion cross section is associated with a resonance. For comparison, the figure shows also the fusion excitation function for the case where the coupling strength has been increased to $\nu^2 = 0.6$ (thin solid line). The Q-value is +4.0 MeV. As is expected, the peak position has shifted toward lower energy.

Figs. 8 and 9 show the absolute values of the effective channel amplitudes corresponding to Fig. 7. Both of them show a resonance peak for a given set of coupling strengths and the reaction Q-value. Clearly, the sum of the squared effective channel amplitudes is not equal to one[18]) (see eq. (5.7)).

7. Summary and Discussion

We have considered a schematic model of heavy ion collisions containing two intrinsic channels, coupled by a δ-function interaction at the top of the potential barrier. We have derived semi-classical expressions for the corresponding S-matrix and of the fusion probability.

The results are particularly simple when there is strong internal absorption. In that case, the coupling Hamiltonian yields a unique barrier-top resonance depending on the reaction Q-value and on the coupling strength in the Hamiltonian. The position of the barrier-top resonance relative to the barrier

height is proportional to the square of the coupling strength and to the curvature of the potential barrier. A peculiar property of the barrier-top resonance is that its leakage width does not involve the barrier penetration factor. Consequently, the width does not change rapidly when the resonance position shifts in energy, unlike the ordinary potential resonances.

Concerning fusion, we found that the sub-barrier fusion cross section is enhanced due to channel coupling. Remarkably, the enhancement occurs not only for positive Q-values, but also for negative Q-values. Also, the fusion excitation function shows a resonance peak at the position where a condition for a barrier-top resonance is fulfilled.

The occurrence of one and only one barrier-top resonance for a given set of the reaction Q-value and the coupling strength can be understood if we remember that a δ-function potential yields always one bound state. If there are n intrinsic channels, we will have $[n/2]$ barrier-top resonances, $[\ ]$ being the Gauss symbol. This can be shown in a model, where the tunneling degree of freedom linearly couples to a degenerate spin system with degeneracy $(2J+1)$[26]. In Ref.27, Lee et al. studied the effects of channel coupling for the model in which the two channel intrinsic Hamiltonian of the present work is replaced by the Hamiltonian for a harmonic oscillator. This model also shows many peaks of barrier-top resonances for a given set of the coupling strength and the oscillator frequency. Clearly, the barrier-top resonance will not show up if the internal absorption extends over the coupling region.

Acknowledgement

This is a joint work with G.F. Bertsch, whom I should like to thank for invaluable discussions and for useful comments in preparing the manuscript. I thank also H. Esbensen and A.B. Balantekin for useful discussions, and acknowledge the support of the National Science Foundation.

Appendix A

The Method of the Comparison Equation

The Schrödinger equation (2.1) is decoupled into two independent one-dimensional Schrödinger equations except for the matching point R_B. We therefore consider a one dimensional differential equation for a complex variable r,

$$\left[\frac{d^2}{dr^2} + \chi(r)\right] \psi(r) = 0 \qquad (A.1)$$

where

$$\chi(r) = \frac{2\mu}{\hbar^2}(E - U(r)) \qquad (A.2)$$

For real values of r, eq. (A.1) is nothing but the Schrödinger equation. Since, however, the turning points, zeroes of $\chi(r)$, are distributed in the complex r-plane for a complex potential, it is more appropriate to consider not the original Schrödinger equation, but its analytic continuation to the complex plane. The region close to the real axis is, of course, the most important.

In the method of the comparison equation, one introduces the following subsidiary equation,

$$\left[\frac{d^2}{d\sigma^2} + \Gamma(\sigma)\right] \phi(\sigma) = 0 \qquad (A.3)$$

The comparison function $\Gamma(\sigma)$ should be chosen such that the solution of eq. (A.3) is known, and that the topological structure of $\chi(r)$ and of $\Gamma(\sigma)$ is equivalent. For example, the number of zeroes of both functions should be identical.

One can prove that the wave function $\psi(r)$ can be well approximated by the solution of the comparison equation $\phi(\sigma)$ as,

$$\psi(r) \approx \left(\frac{d\sigma}{dr}\right)^{-\frac{1}{2}} \phi(\sigma) \tag{A.4}$$

if the mapping from the r-space to the σ-space is defined as

$$\frac{d\sigma}{dr} = \left[\frac{\chi(r)}{\Gamma(\sigma)}\right]^{\frac{1}{2}} \tag{A.5}$$

i.e. if the mapping conserves the action integral. Clearly, it is required that the zeroes of $\chi(r)$ are mapped onto the zeroes of $\Gamma(\sigma)$.

We use different mapping functions for the barrier region, including regions I and II in the text, and for the internal region, i.e. region III in the text. A convenient comparison function for the barrier region is a parabolic function,

$$\Gamma^{(1)}(\sigma) = \frac{1}{4}\sigma^2 - \xi \tag{A.6}$$

The mapping equation (A.6) leads to,

$$\xi = \frac{i}{\pi}\int_{r_1}^{r_2} [\chi(r)]^{\frac{1}{2}}\, dr \tag{A.7}$$

For the internal region, a linear function is the approximate comparison function,

$$\Gamma^{(2)}(\sigma) = C(\sigma - \sigma_3) \tag{A.8}$$

where c is any constant.

Appendix B

Convenient Basis Wave Functions for a Quadratic Potential Barrier

The comparison equation (A.3) is Weber's equation[22] when the comparison function is a parabolic function as given by eq. (A.6). Two independent solutions are the Whittaker functions $D_{(i\varepsilon-\frac{1}{2})}(e^{\frac{1}{4}i\pi}\sigma)$ and $D_{(-i\varepsilon-\frac{1}{2})}(e^{-\frac{1}{4}i\pi}\sigma)$, or any of their linear combinations. It is convenient to choose the linear combination such that the resultant wave functions asymptotically behave as either an incoming wave or an outgoing wave,

$$\begin{pmatrix} \phi_{IW}^{(k)}(\xi,\sigma) \\ \phi_{OW}^{(k)}(\xi,\sigma) \end{pmatrix} = \begin{pmatrix} b_{11}^{(k)} & b_{12}^{(k)} \\ b_{21}^{(k)} & b_{22}^{(k)} \end{pmatrix} \begin{pmatrix} D_{(i\varepsilon-\frac{1}{2})}(e^{\frac{1}{4}i\pi}\sigma) \\ D_{(-i\varepsilon-\frac{1}{2})}(e^{-\frac{1}{4}i\pi}\sigma) \end{pmatrix} \tag{B.1}$$

The asymptotic forms of the Whittaker functions $D_n(z)$ depend on the argument of z, so that the coefficients of the linear combination, the matrix b, have to be chosen separately for the right and for the left sides of the potential barrier. The upper suffix k has been introduced in this connection to specify either R- or L-side of the potential barrier.

The asymptotic behaviour of the Whittaker function is discussed in the textbook of Whittaker and Watson. Using the formulae there, one learns that the appropriate matrices $b^{(k)}$ are

$$\begin{pmatrix} \ell_{11}^{(L)} & \ell_{12}^{(L)} \\ \ell_{21}^{(L)} & \ell_{22}^{(L)} \end{pmatrix} = \begin{pmatrix} \frac{\sqrt{2\pi}}{\Gamma(\frac{1}{2}+i\ell)}\, e^{\frac{3}{4}\pi\ell}\, e^{\frac{3}{8}\pi i} & e^{\frac{3}{4}\pi\ell}\, e^{-\frac{3}{8}\pi i} \\ e^{-\frac{5}{8}\pi\ell}\, e^{\frac{3}{8}\pi i} & \frac{\sqrt{2\pi}}{\Gamma(\frac{1}{2}-i\ell)}\, e^{\frac{3}{4}\pi\ell}\, e^{-\frac{3}{8}\pi i} \end{pmatrix} \qquad \text{(B.2)}$$

and

$$\begin{pmatrix} \ell_{11}^{(R)} & \ell_{12}^{(R)} \\ \ell_{21}^{(R)} & \ell_{22}^{(R)} \end{pmatrix} = \begin{pmatrix} e^{\frac{3}{8}\pi i}\, e^{\frac{1}{4}\pi\ell} & 0 \\ 0 & e^{-\frac{3}{8}\pi i}\, e^{\frac{1}{4}\pi\ell} \end{pmatrix} \qquad \text{(B.3)}$$

One can easily confirm that the resultant wave functions ψ_{Iw} and ψ_{Ow} then have indeed the following desired asymptotic behaviour,

$$\begin{pmatrix} \psi_{Iw}^{(L)}(r) \\ \psi_{Ow}^{(L)}(r) \end{pmatrix} \sim \frac{1}{\sqrt{2}}[\chi(r)]^{-\frac{1}{4}} \begin{pmatrix} e^{-iS_2(r)}\, e^{-i\frac{1}{2}\ell\ln\ell/e}\, e^{\frac{1}{4}\pi i} \\ e^{iS_1(r)}\, e^{i\frac{1}{2}\ell\ln\ell/e}\, e^{-\frac{1}{4}\pi i} \end{pmatrix} \qquad \text{(B.4)}$$

and

$$\begin{pmatrix} \psi_{Iw}^{(R)}(r) \\ \psi_{Ow}^{(R)}(r) \end{pmatrix} \sim \frac{1}{\sqrt{2}}[\chi(r)]^{-\frac{1}{4}} \begin{pmatrix} e^{-i[S_1(r)-\frac{1}{2}\ell\ln\ell/e-\frac{\pi}{4}]} \\ e^{i[S_1(r)-\frac{1}{2}\ell\ln\ell/e-\frac{\pi}{4}]} \end{pmatrix} \qquad \text{(B.5)}$$

where

$$S_i(r) = \int_{r_i}^{r} [\chi(r)]^{\frac{1}{2}}\, dr \qquad \text{(B.6)}$$

In deriving eqs. (B.4) and (B.6), we have used the following solutions of the mapping equation eq. (A.5),

$$\int_{r_2}^{r} [\chi(r)]^{\frac{1}{2}}\, dr = -\left\{\frac{\sigma^2}{4} + \frac{1}{2}\ell\ln\ell/e - \ell\ln(-\sigma)\right\} \qquad \text{(B.7)}$$

(if $r < r_2$, i.e. if $\sigma < \sigma_2$)

and

$$\int_{r_1}^{r} [\chi(r)]^{\frac{1}{2}}\, dr = \frac{1}{4}\sigma^2 + \frac{1}{2}\ell\ln\ell/e - \ell\ln\sigma \qquad \text{(B.8)}$$

(if $r > r_1$, i.e. if $\sigma > \sigma_1$)

Appendix C

Two Level Degenerate Model

In this appendix, we consider a two level, degenerate model. It clearly demonstrates the importance of the potential renormalization in the problem of quantum tunneling in multi-dimensional systems.

C.1. POTENTIAL RENORMALIZATION

Let us denote the degenerate intrinsic energy as ϵ_0. Eq. (2.1) then becomes

$$\left\{-\frac{\hbar^2}{2\mu}\frac{d^2}{dr^2}+U(r)\right\}\begin{pmatrix}1&0\\0&1\end{pmatrix}\Psi+\epsilon_0\begin{pmatrix}1&0\\0&1\end{pmatrix}\Psi+\lambda f(r)\sigma_x\Psi=E\begin{pmatrix}1&0\\0&1\end{pmatrix}\Psi \qquad (C.1)$$

This equation can be easily decoupled by using a unitary matrix M given by

$$M=\begin{pmatrix}1&1\\-1&1\end{pmatrix} \quad \text{and} \quad M^{-1}=\frac{1}{2}\begin{pmatrix}1&-1\\1&1\end{pmatrix} \qquad (C.2)$$

The result reads

$$\begin{pmatrix}-\frac{\hbar^2}{2\mu}\frac{d^2}{dr^2}+U(r)+\lambda f(r) & 0\\ 0 & -\frac{\hbar^2}{2\mu}\frac{d^2}{dr^2}+U(r)-\lambda f(r)\end{pmatrix}\Phi=(E-\epsilon_0)\begin{pmatrix}1&0\\0&1\end{pmatrix}\Phi \qquad (C.3)$$

where

$$\Phi=M\Psi=\begin{pmatrix}\varphi_1&0\\0&\varphi_2\end{pmatrix} \qquad (C.4)$$

The problem thus reduces to quantum tunneling through one dimensional effective potential barrier $U_1^{(eff)}(r) = U(r) + \lambda f(r)$ or $U_2^{(eff)}(r) = U(r) - \lambda f(r)$. Figs. 10 and 11 show the effective

potential barrier for two typical kinds of coupling form factor. They clearly demonstrate the importance of the potential renormalization and the sensitivity of the potential renormalization to the property of the coupling form factor. Only one of the quantum tunneling, either through the effective potential barrier $U_1^{(eff)}(r)$ or through $U_2^{(eff)}(r)$, which provides a smaller potential barrier, will dominate under certain circumstances. If the coupling form factor is localized around the barrier region, as shown in Fig. 11, and if the coupling is so strong that the effective potential produces resonant states, then the excitation function of the tunneling probability will show peaks at the resonance energies. The δ-function coupling is a typical example of such cases.

C.2. TRANSMISSION AMPLITUDES FOR A GENERAL COUPLING FORM FACTOR

By inverting eq. (C.4), we obtain

$$\Psi=\frac{1}{2}\begin{pmatrix}\varphi_1-\varphi_2\\ \varphi_1+\varphi_2\end{pmatrix} \qquad (C.5)$$

Let us consider the wave function ϕ_i and denote the amplitudes of the incoming and of the outgoing waves on the right hand side of the potential barrier as $C_{iR}^{(-)}$ and $C_{iR}^{(+)}$, respectively, and the amplitude of the ingoing wave on the left hand side of the potential barrier as $C_{iL}^{(-)}$ (see Fig. 12). Eq. (C.5) then shows that the wave function ψ has the following asymptotic behaviour. On the right hand side of the potential barrier,

$$\frac{1}{2}\begin{pmatrix} \{C_{1R}^{(-)} - C_{2R}^{(-)}\} e^{-ikR} + \{C_{1R}^{(+)} - C_{2R}^{(+)}\} e^{ikR} \\ \{C_{1R}^{(-)} + C_{2R}^{(-)}\} e^{-ikR} + \{C_{1R}^{(+)} + C_{2R}^{(+)}\} e^{ikR} \end{pmatrix} \qquad (C.6)$$

whereas, on the left hand side,

$$\frac{1}{2}\begin{pmatrix} \{C_{1L}^{(-)} - C_{2L}^{(-)}\} e^{-ikR} \\ \{C_{1L}^{(-)} + C_{2L}^{(-)}\} e^{-ikR} \end{pmatrix} \qquad (C.7)$$

Assume that the system was initially in the first channel. Eq. (C.6) shows that this initial condition requires

$$C_{2R}^{(-)} = -C_{1R}^{(-)} \qquad (C.8)$$

If we represent the transmission amplitude in the process where the system is in the i-th channel when the tunneling process has been completed as $A^{(i)}$, eqs. (C.6) through (C.8) lead to,

$$A^{(1)} = \frac{C_{1L}^{(-)} - C_{2L}^{(-)}}{C_{1R}^{(-)} - C_{2R}^{(-)}} = \frac{1}{2}\left\{\frac{C_{1L}^{(-)}}{C_{1R}^{(-)}} + \frac{C_{2L}^{(-)}}{C_{1R}^{(-)}}\right\} = \frac{1}{2}(a_1 + a_2) \qquad (C.9)$$

and

$$A^{(2)} = \frac{C_{1L}^{(-)} + C_{2L}^{(-)}}{C_{1R}^{(-)} - C_{2R}^{(-)}} = \frac{1}{2}\left\{\frac{C_{1L}^{(-)}}{C_{1R}^{(-)}} - \frac{C_{2L}^{(-)}}{C_{2R}^{(-)}}\right\} = \frac{1}{2}(a_1 - a_2) \qquad (C.10)$$

Each transmission coefficient a_i can be easily calculated by solving the one dimensional quantum tunneling for the effective potential $U_i^{(eff)}(r)$.

C.3. TRANSMISSION AMPLITUDES FOR δ-FUNCTION COUPLING

Let us consider a special two level degenerate model, in which the original tunneling potential barrier is parabolic, and where the coupling occurs only at the barrier top position, i.e. when $f(r) = \delta(r - R_B)$. In this case, the transmission amplitudes $\{a_i\}$ for the quantum tunneling through the decoupled effective potential barriers $U_i^{(eff)}(r)$, i = 1,2, are explicitly given by

$$a_1 = t_1 \frac{1}{1 + \nu f(\varepsilon, \varepsilon)} \qquad (C.11)$$

and

$$a_2 = t_1 \frac{1}{1 - \nu f(\varepsilon, \varepsilon)} \qquad (C.12)$$

where t_1 is the transmission amplitude through the bare parabolic potential barrier.

The transmission amplitudes $\{A_i\}_{i=1,2}$ are then given by

$$A^{(1)} = \frac{1}{2} t_1 \left\{\frac{1}{1 + \nu f(\varepsilon, \varepsilon)} + \frac{1}{1 - \nu f(\varepsilon, \varepsilon)}\right\} \qquad (C.13a)$$

$$= t_1 \frac{1}{1 - \nu^2 [f(\varepsilon, \varepsilon)]^2} \qquad (C.13b)$$

and

$$A^{(2)} = \frac{1}{2} t_1 \left\{ \frac{1}{1 + \nu f(\xi,\xi)} - \frac{1}{1 - \nu f(\xi,\xi)} \right\} \qquad \text{(C.14a)}$$

$$= - t_1 \frac{\nu f(\xi,\xi)}{1 - \nu^2 [f(\xi,\xi)]^2} \qquad \text{(C.14b)}$$

Eqs. (C.13) and (C.14) agree with the zero Q-value limit of the transmission amplitudes obtained for general Q-values. This way to derive the tunneling probability clearly indicates that the final tunneling probability has peaks at the energies where one of the effective potentials has resonances.

References

1. R.G. Stockstad et al., Phys. Rev. Lett. 41 (1978) 465; Phys. Rev. C21 (1980) 2427; Z. Phys. A295 (1980) 269.
2. U. Jahnke et al., Phys. Rev. Lett. 48 (1982) 17.
3. W. Reisdorf et al., Phys. Rev. Lett. 49 (1982) 1811.
4. M. Beckerman et al., Phys. Rev. C23 (1981) 1581; C25 (1982) 837; C28 (1983) 1963; Phys. Rev. Lett. 45 (1980) 1472; 50 (1983) 471.
5. W.S. Freeman et al., Phys. Rev. Lett. 50 (1983) 1563.
6. G.M. Berkowitz and P. Braun-Munzinger, Phys. Rev. C28 (1983) 667.
7. R. Pengo et al., Nucl. Phys. A411 (1983) 255.
8. H. Esbenson, Nucl. Phys. A352 (1981) 147.
9. S. Landowne and J.R. Nix, Nucl. Phys. A368 (1981) 352.
10. L.C. Vaz, J.M. Alexander, and G.R. Satchler, Phys. Rep. C69 (1981) 374.
11. R. Broglia, A. Winther et al., Phys. Rev. C27 (1983) 2433; Nucl. Phys. A409 (1983) 163C; Nucl. Phys. A405 (1983) 381; A407 (1983) 221; Phys. Lett. 133B (1983) 34.
12. H. Esbensen, J.Q. Wu, and G.F. Bertsch, Nucl. Phys. A411 (1983) 275.
13. H.J. Krappe, K. Möhring, M.C. Nemes, and H. Rossner, Hahn-Meitner Institute, preprint 1983.
14. P.M. Jacobs and U. Smilansky, Phys. Lett. 127B (1983) 313.
15. S.Y. Lee and N. Takigawa, Phys. Rev. C28 (1983) 1123.
16. N. Takigawa and G.F. Bertsch, Phys. Rev. C (submitted).

17. N. Takigawa and G.F. Bertsch, to be published.

18. S.Y. Lee, preprint, SUNY, 1983.

19. D.M. Brink and N. Takigawa, Nucl. Phys. A279 (1977) 159.

20. S.Y. Lee and N. Takigawa, Nucl. Phys. A308 (1978) 189.

21. M. Abramowitz and I.A. Stegun, Handbook of Mathematical Functions (Dover, 1972), p. 451.

22. E.T. Whittaker and J.N. Watson, A Course of Modern Analysis (Cambridge University Press, 1963), p. 347.

23. M.V. Berry and K.E. Mount, Rep. Prog. Phys. 35 (1972) 315.

24. W.A. Friedman and C.J. Goebel, Ann. of Phys. 104 (1977) 145.

25. S.Y. Lee, N. Takigawa and C. Marty, Nucl.Phys. A308 (1978) 161.

26. A.B. Balantekin and N. Takigawa, to be published.

27. S.Y. Lee, M. Prakash, L.C. Vaz and J. Alexander, preprint, SUNY, 1983.

Figure Captions

Fig. 1. Illustration of the two channel barrier top δ-function coupling model.

Fig. 2. The absolute values of the S-matrix elements as functions of the incident energy are shown for different values of the coupling strength. The thin and the thick lines are $|n_{11}|$ and $|n_{12}|$ respectively. The value of the squared coupling strength ν^2 is 0.2, 0.6, and 1.0 for the solid, the dashed, and the dot-dashed lines, respectively. The Q-value is zero.

Fig. 3. The energy where the S-matrix elements show resonance extrema is plotted as a function of the squared coupling strength. The dot-dashed line is the prediction of the semi-classical theory eq. (4.6) together with eq. (4.8). The Q-value is equal to zero.

Fig. 4. The absolute values of the S matrix elements as functions of the incident energy are shown for different Q-values. The thin and the thick lines are $|n_{11}|$ and $|n_{12}|$, respectively. The Q-value for the solid, the dot-dashed, and the dashed lines is +4 MeV, 0 MeV, and -4 MeV, respectively. The coupling strength has been fixed to be $\nu^2 = 0.4$.

Fig. 5. Excitation function of the fusion cross section. The numbers denote the values of the squared coupling strength ν^2. The Q-value is equal to zero. The monotonic line represents the bare tunneling probability.

Fig. 6. The absolute value of the effective channel amplitude $|h_1|$ is plotted as a function of the incident energy. The numbers are the values of the squared coupling strength. The Q-value is zero.

Fig. 7. The excitation function of the fusion cross section. The thick lines denoted by a are for $\nu^2 = 0.4$, while the thin solid line denoted by b for $\nu^2 = 0.6$. The lower suffix of a and b represent the Q-value. The thick monotonic curve is the bare tunneling probability.

Fig. 8. Dependence of the absolute value of the effective entrance channel amplitude $|h_1|$ on the Q-value, and on the coupling strength. The notations are the same as in Fig. 7.

Fig. 9. The same as Fig. 8, but for $|h_2|$.

Fig. 10. Effective potential barrier in a degenerate two channel model.

Fig. 11. Effective potential barrier in a degenerate two channel model.

Fig. 12. Amplitudes of a channel wave function in the presence of strong internal absorption.

MSU-84-054

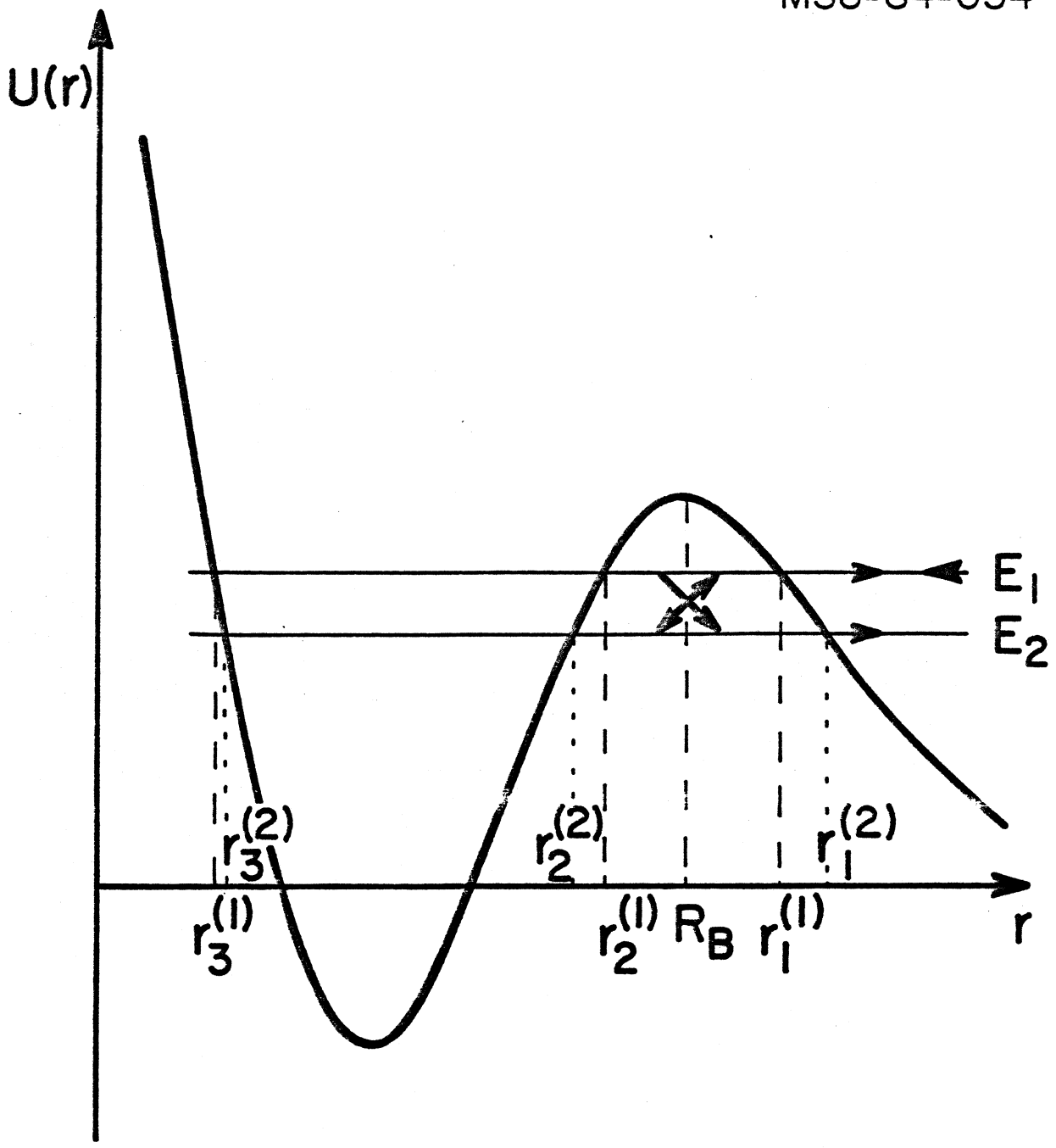

Fig. 1

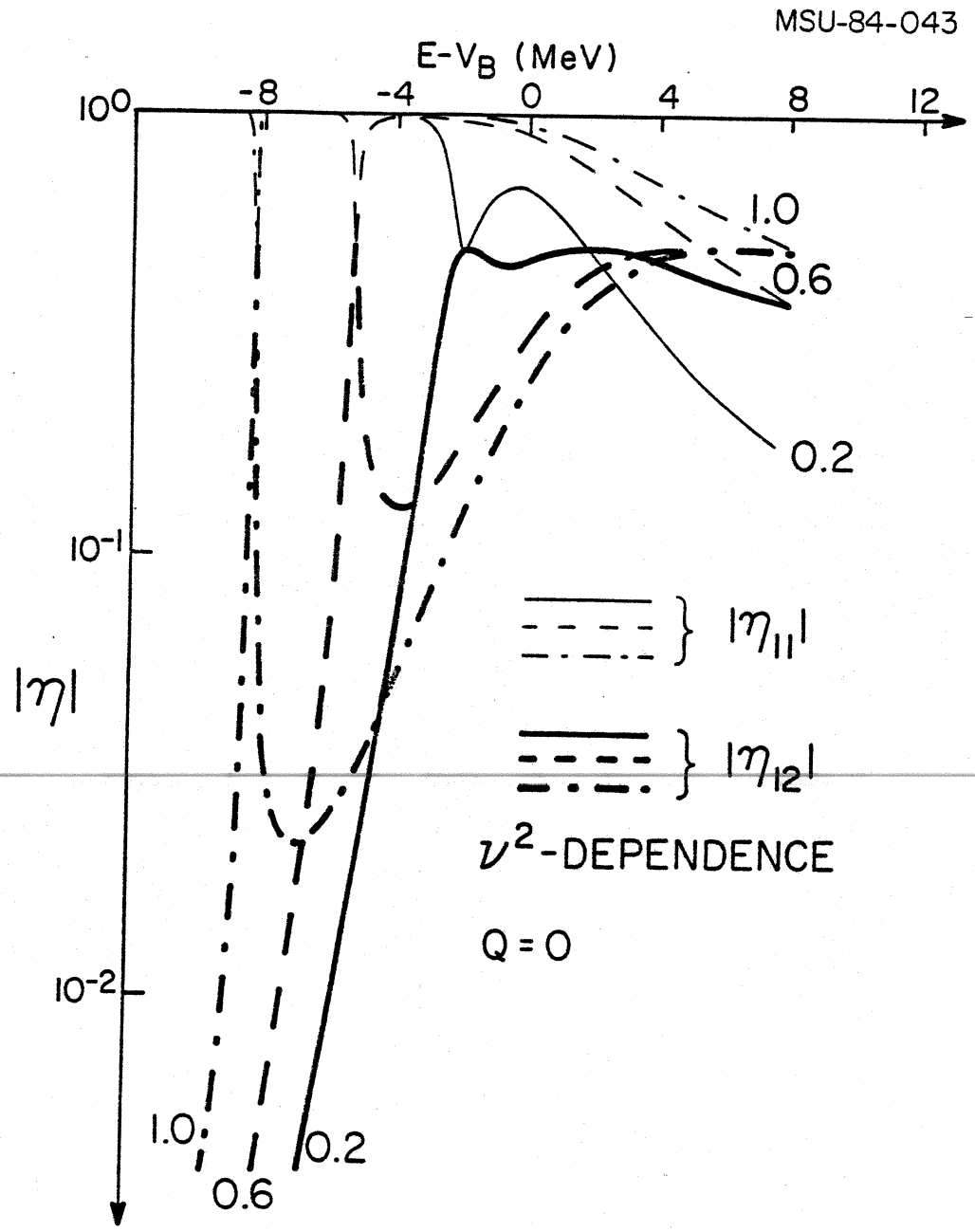
MSU-84-043
E-V_B (MeV)
-8
-4
0
4
8
12
10^0
10^-1
10^-2
|η|
1.0
0.6
0.2
|η11|
|η12|
ν²-DEPENDENCE
Q = 0
1.0
0.6
0.2

Fig. 2

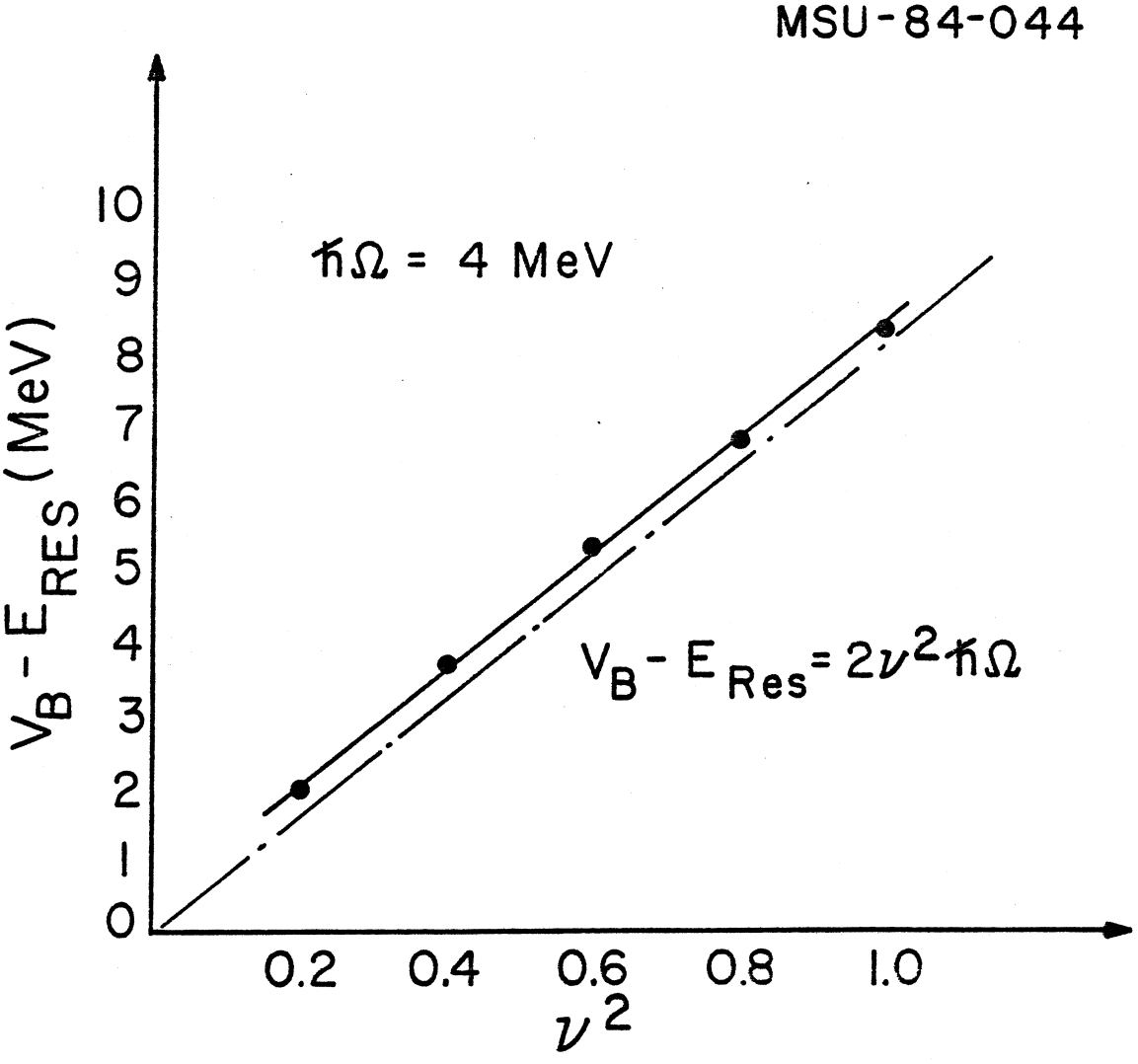
MSU-84-044
$\hbar\Omega$ = 4 MeV
$V_B - E_{RES}$ (MeV)
$V_B - E_{Res} = 2\nu^2\hbar\Omega$
0
1
2
3
4
5
6
7
8
9
10
0.2
0.4
0.6
0.8
1.0
ν^2

Fig. 3

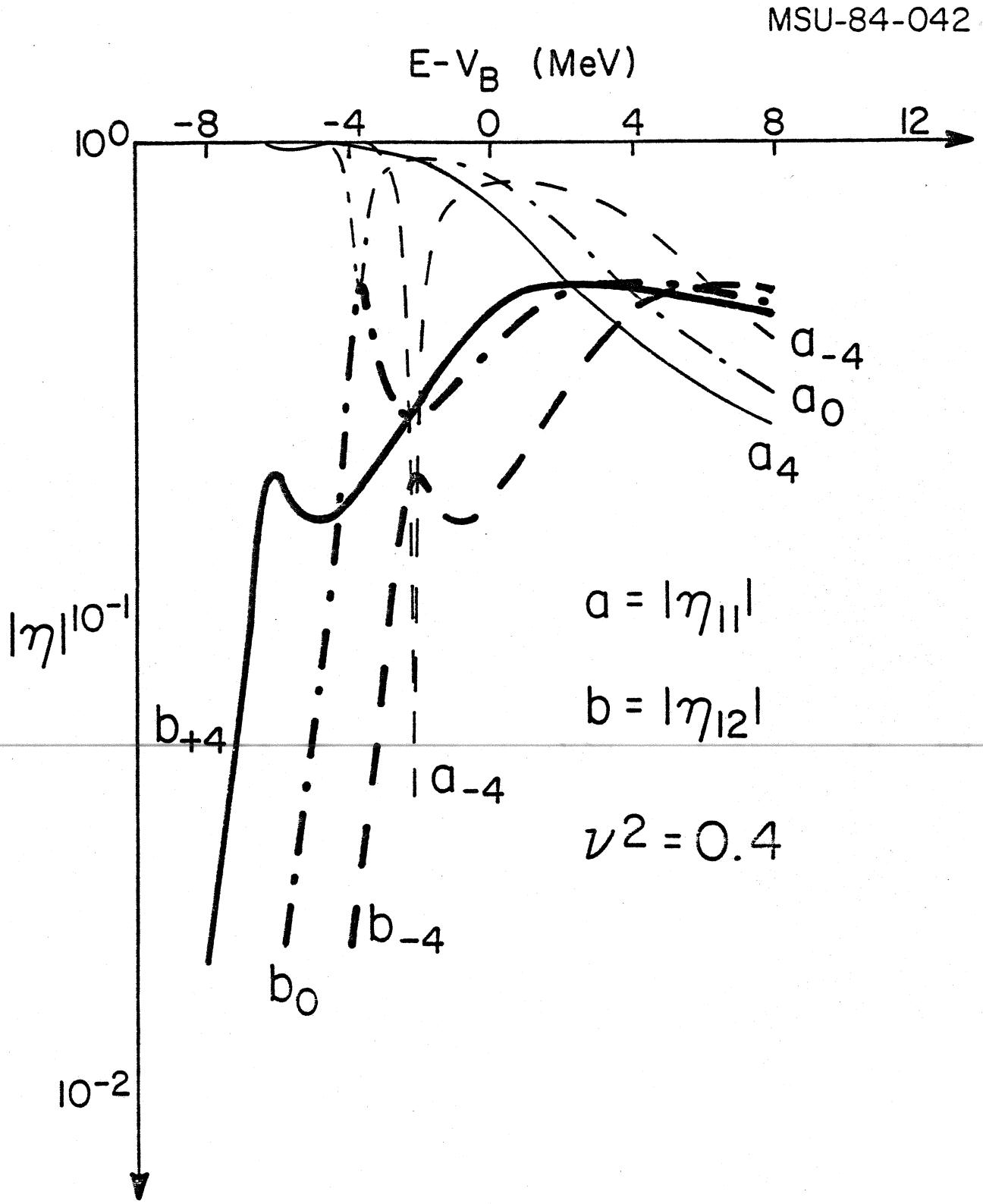
MSU-84-042
E-V_B (MeV)
-8
-4
0
4
8
12
10^0
|η|
10^-1
10^-2
a_-4
a_0
a_4
a = |η11|
b = |η12|
b_+4
|a_-4
ν^2 = 0.4
b_-4
b_0

Fig. 4

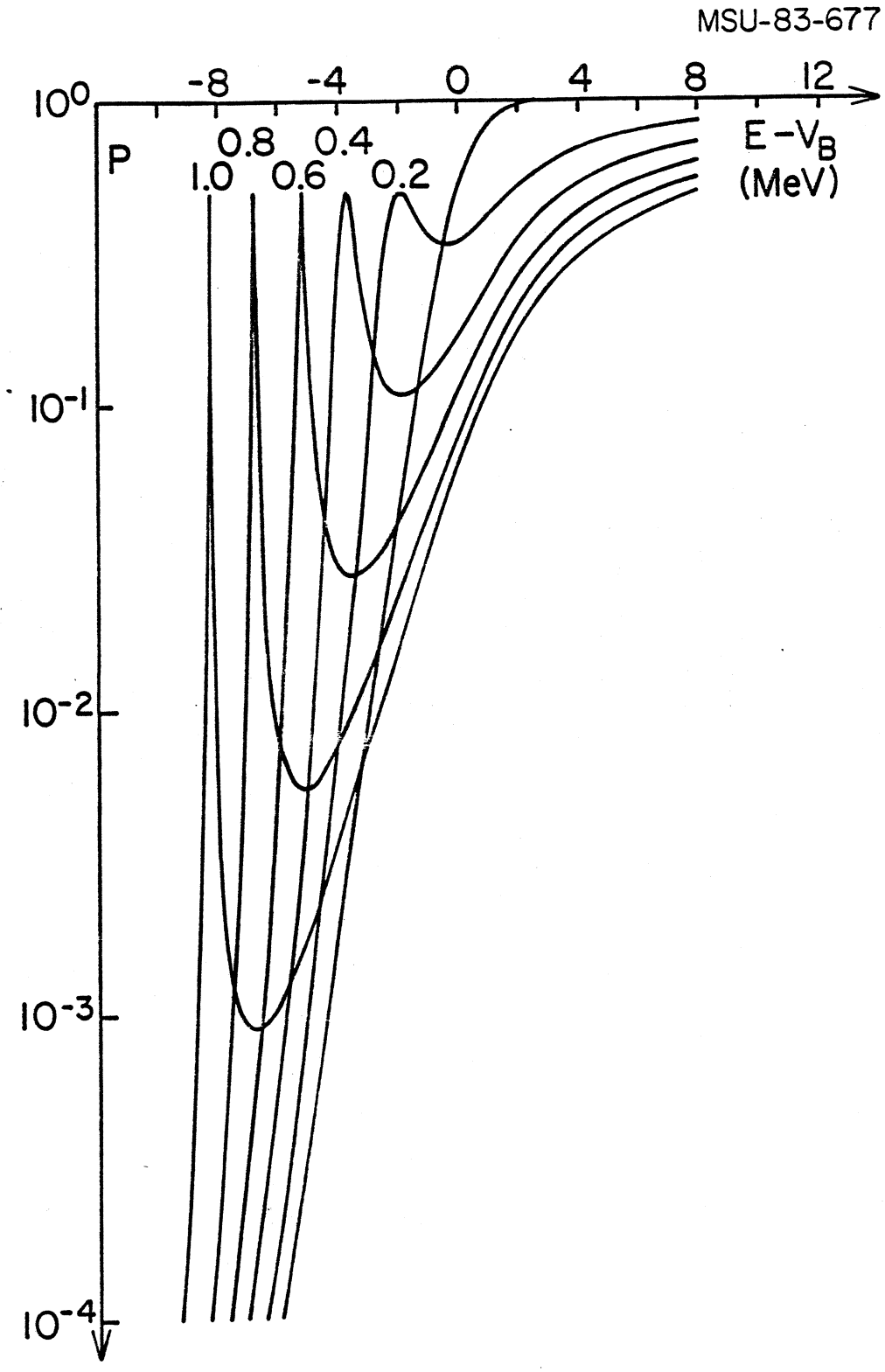

Fig. 5

MSU-83-676

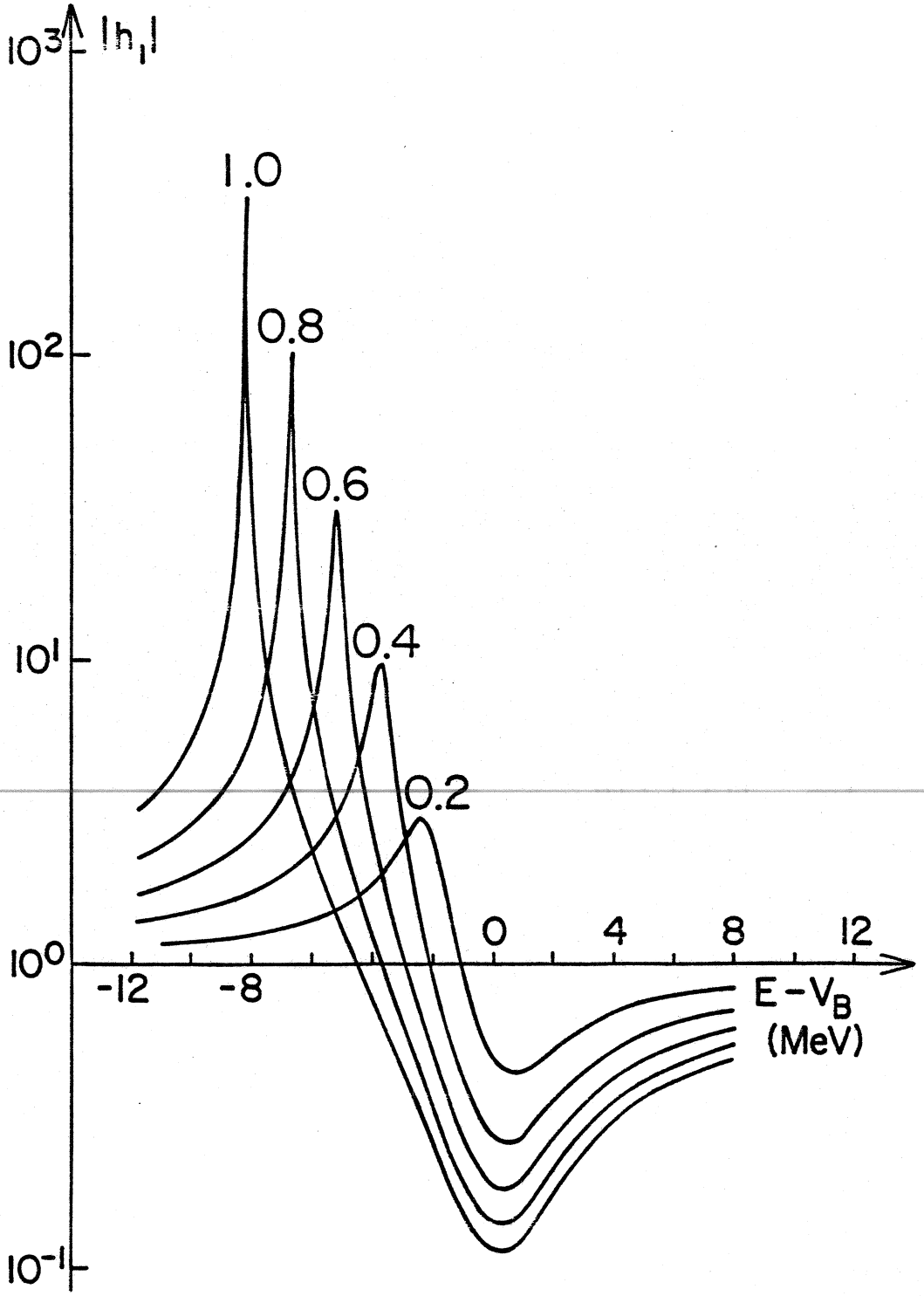

Fig. 6

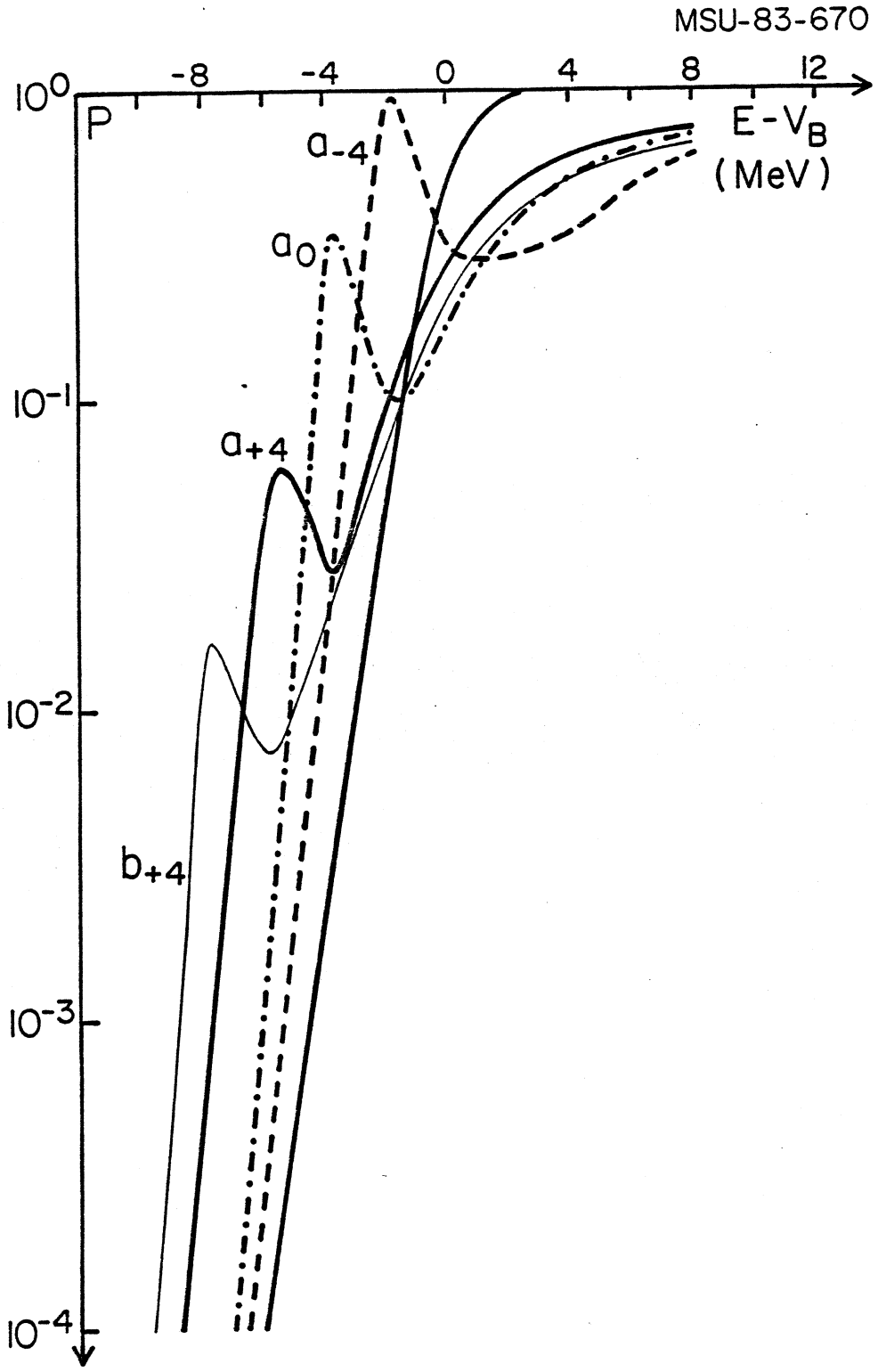

Fig. 7

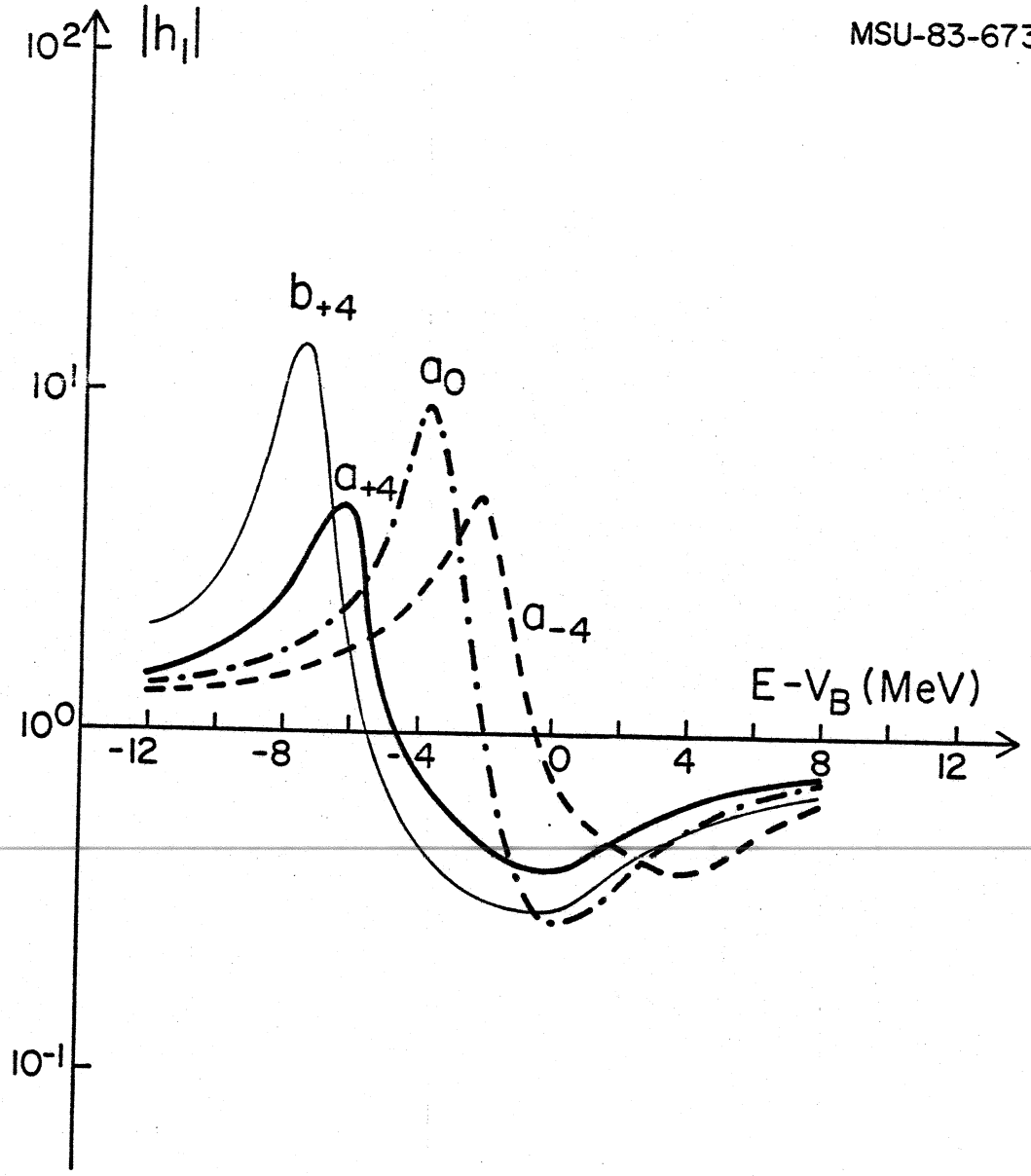

Fig. 8

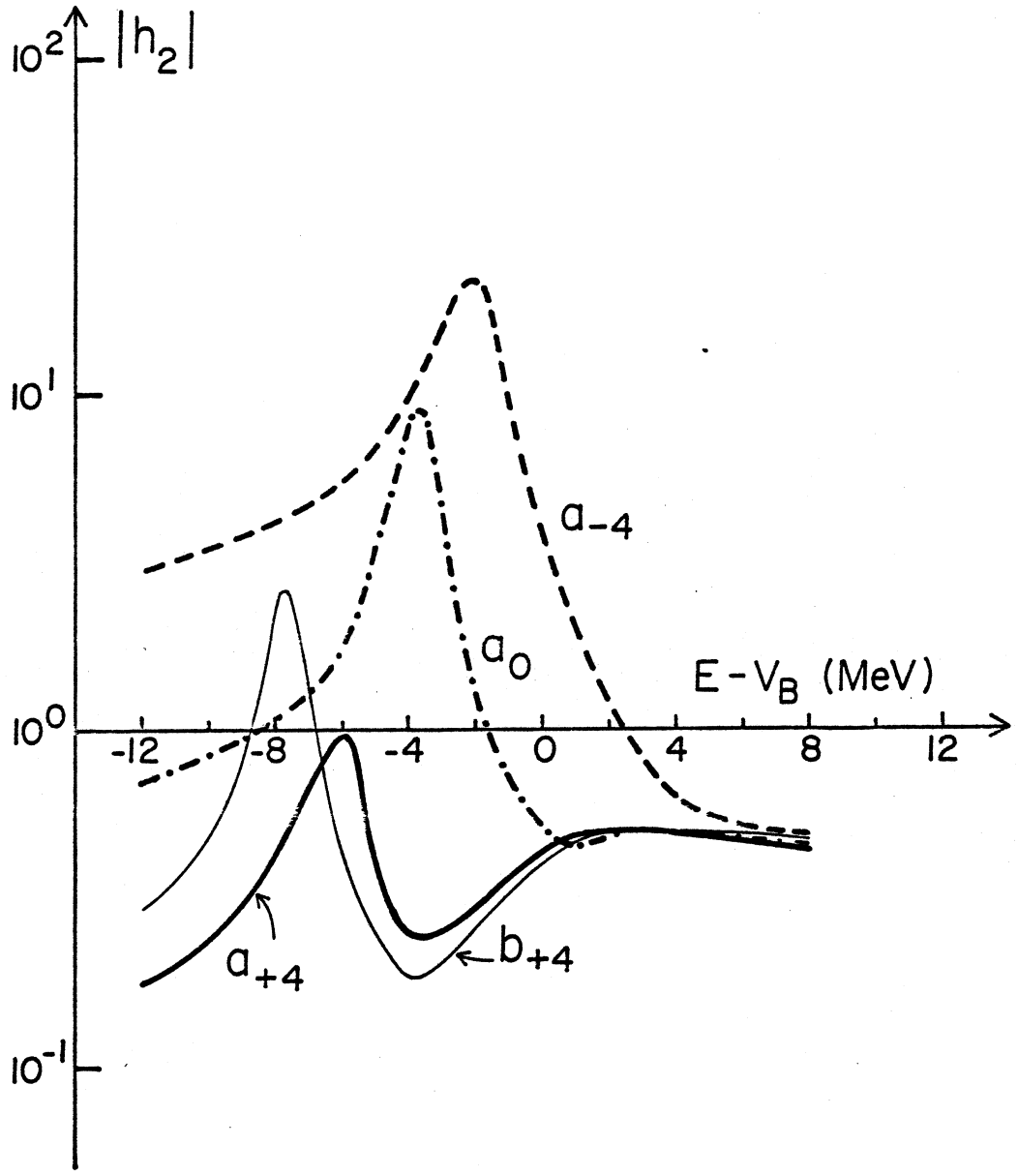

Fig. 9

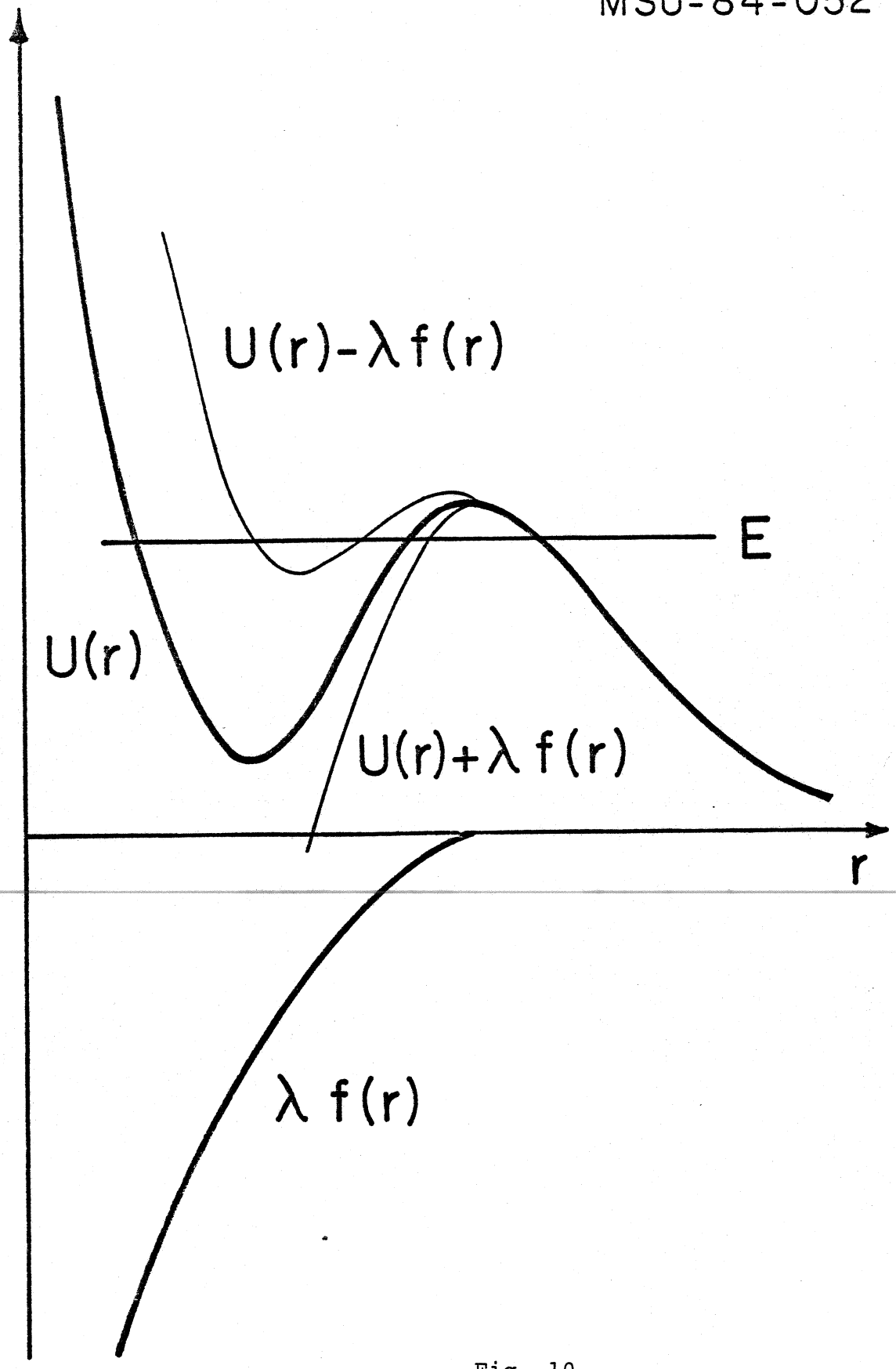

Fig. 10

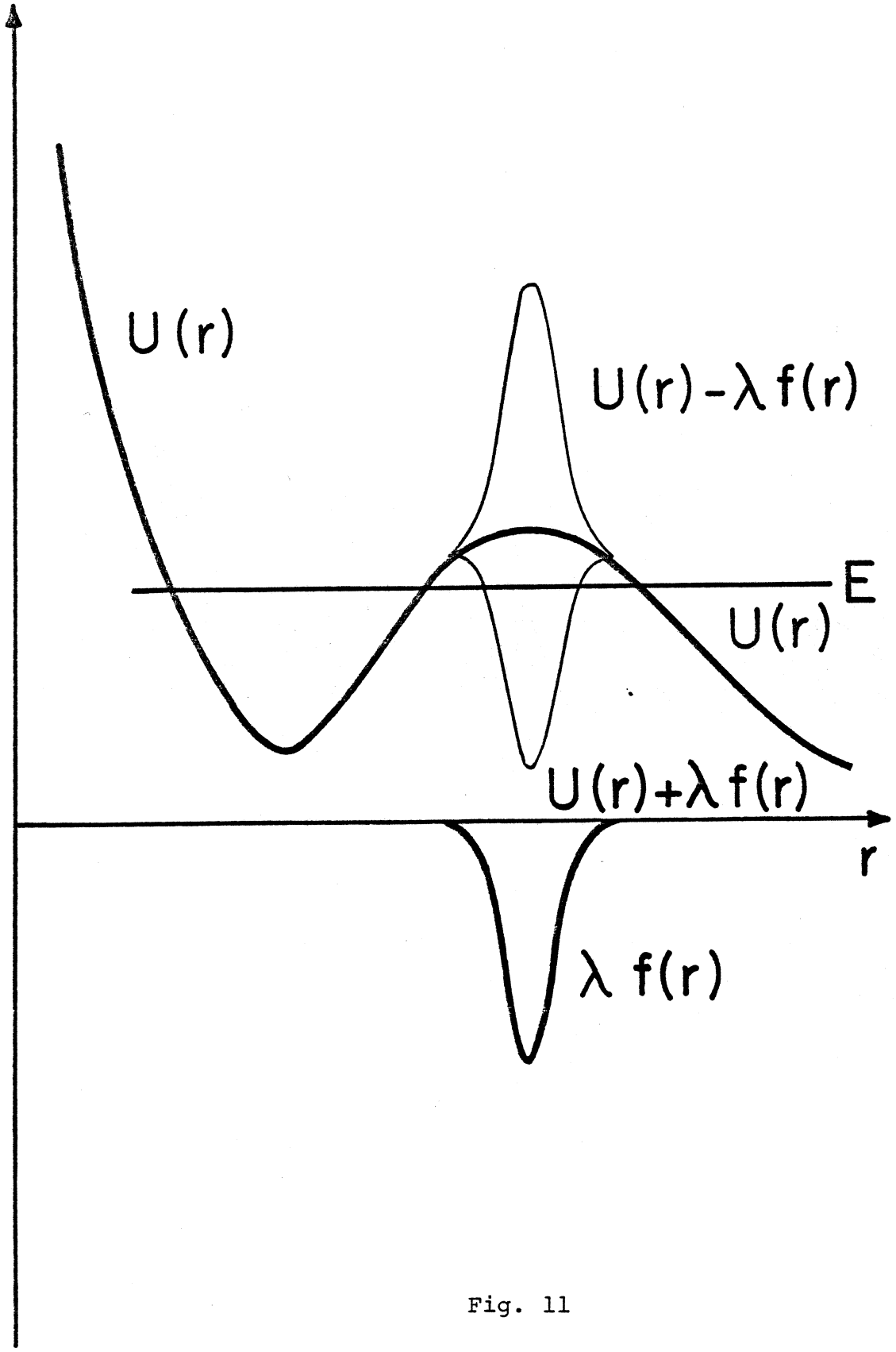

Fig. 11

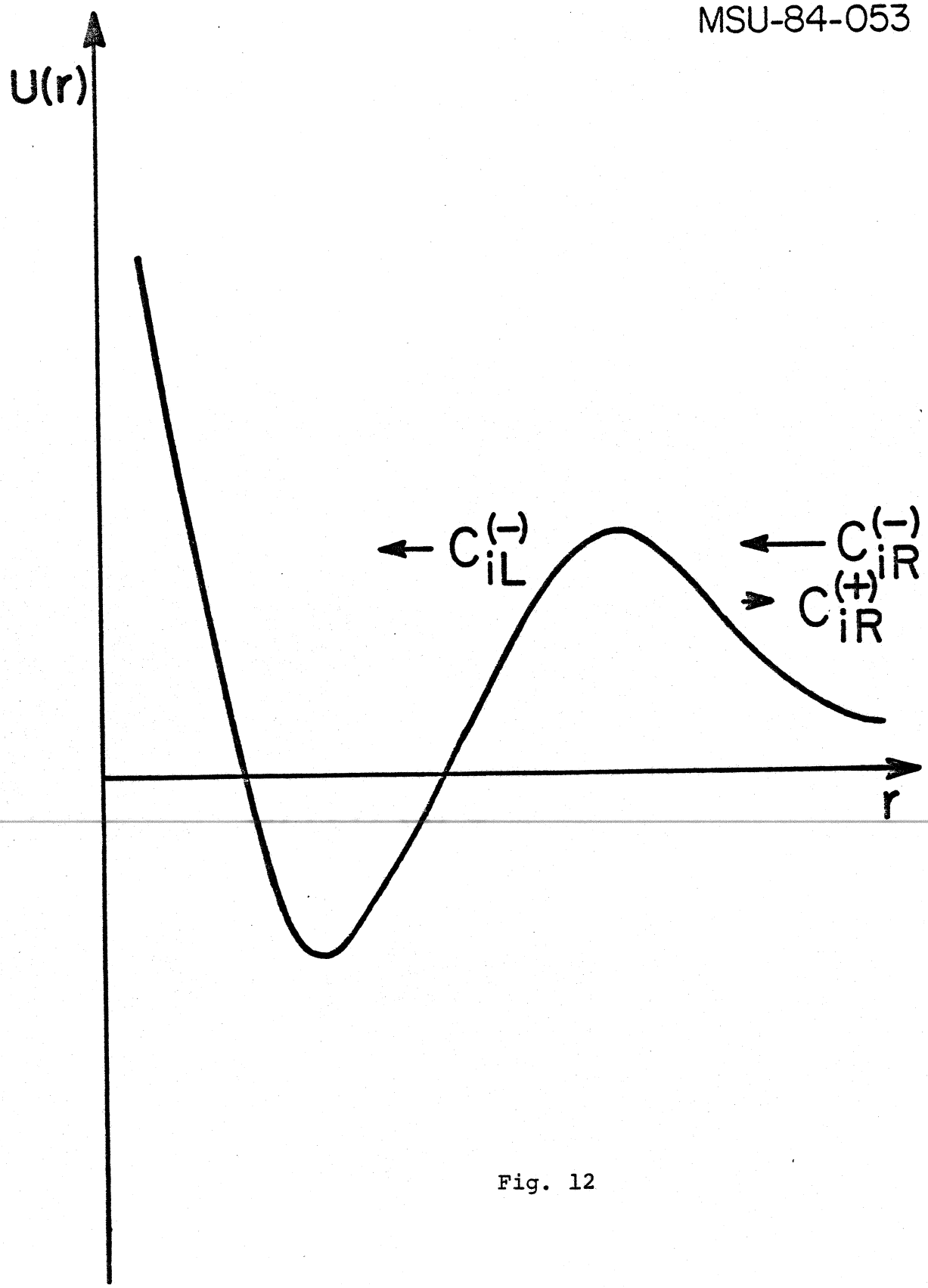

Fig. 12